

9609

Prepared for:

Min. Vlaamse Gemeenschap, Department LIN

## Cohesive sediment transport model for the Lower Sea Scheldt

Steps for set-up and further development

Report

June 2004

030504

Z2516-88

**wl | delft hydraulics**

0307 014 919X



Prepared for:

Min. Vlaamse Gemeenschap, Department LIN

## Cohesive sediment transport model for the Lower Sea Scheldt

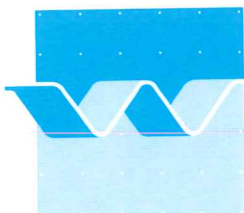
Steps for set-up and further development

C. Kuijper

J.C. Winterwerp

Report

June 2004



**wl | delft hydraulics**



CLIENT: Ministerie Vlaamse Gemeenschap.  
Department LIN.

TITLE: Cohesive sediment transport model for the Lower Sea Scheldt.  
Steps for set-up and further development.

**ABSTRACT:**

The managing authorities of the Lower Sea Scheldt in Belgium have to decide on various measures to guarantee standards on safety, transport and water quality issues in the area. The fate of fine-grained cohesive sediments forms a crucial role in many of the managerial questions and the availability of a predictive tool in these matters is urgently requested. In this report the necessary steps have been described to arrive at an operational numerical model, which can be utilized to assess siltation rates and sediment distribution in access channels. Furthermore, the model should be capable to address the effects of mitigating measures, like passive devices, in reducing siltation rates.

The Lower Sea Scheldt is located in the mixing zone of the Scheldt estuary, which implies that the hydrodynamics are governed by the interaction of (fresh) river and (salt) sea water, resulting in density-induced gravity currents. Along with the complicated geometry and the tidal effects, this results in a three-dimensional flow pattern, which should be modelled according to a three-dimensional approach for the area of interest. Boundary conditions at the upper boundary (at Schelle) and the lower boundary (near Waarde) will be derived from an overall model.

The modelling of the dynamics of cohesive sediments requires an adequate description of the transport cycle, such as: horizontal transport, flocculation, settling and deposition, consolidation and erosion. Many of these aspects are still subject to research and as such a phased approach for the set-up of a cohesive sediment transport model is proposed. During Phase 1, already implemented formulations will be used and the DELFT3D SED ON-LINE model, equipped with state-of-the-art process formulations, will be set up for the Lower Sea Scheldt in conjunction with the WAQUA SCALWEST2000 model, as part of the SIMONA environment, coupled with WAQ. For both models grid schematisations of the areas already exist. Following calibration and validation of the DELFT3D model and the application of the model in answering managerial questions new process formulations, as described in this report, will be implemented as part of Phase 2 of the project. The overall model, covering the Western Scheldt incl. Voordelta, Lower Sea Scheldt and upper reaches of the Scheldt river, will be based on WAQUA/TRIWAQ + WAQ, or alternatively WAQUA/TRIWAQ + SLIB3D.

REFERENCES: bestek nr. 16EB/01/01

VER.	ORIGINATOR	DATE	REMARKS	REVIEW	APPROVED BY
1.0	C. Kuijper	12 february 2004		J.C. Winterwerp	W.M.K. Tilmans
2.0	C. Kuijper	7 juni 2004		J.C. Winterwerp	W.M.K. Tilmans

PROJECT IDENTIFICATION: Z2516-88

KEYWORDS: Lower Sea Scheldt, cohesive sediment, numerical modelling

NUMBER OF PAGES 49

CONFIDENTIAL:  YES, until (date) 2010  NO

STATUS:  PRELIMINARY  DRAFT  FINAL

## Contents

<b>1</b>	<b>Introduction .....</b>	<b>1—1</b>
1.1	Background and objective of the study .....	1—1
1.2	Set up of the study .....	1—1
1.3	Managerial questions.....	1—2
1.4	Contents of this report .....	1—3
<b>2</b>	<b>Large-scale processes in the Lower Sea Scheldt .....</b>	<b>2—1</b>
2.1	The Scheldt basin and Scheldt estuary .....	2—1
2.2	Hydrodynamics .....	2—3
2.2.1	River discharge.....	2—3
2.2.2	Vertical and horizontal tide.....	2—3
2.2.3	Tidal asymmetry .....	2—4
2.2.4	Salinity intrusion .....	2—4
2.2.5	Gravitational circulation.....	2—4
2.3	Sediment dynamics.....	2—5
2.3.1	Input of fluvial/terrestrial sediment .....	2—5
2.3.2	Input of marine sediment.....	2—8
2.3.3	Mixing ratios of fluvial and marine sediments .....	2—10
2.3.4	Bed sediment .....	2—11
2.3.5	Suspended sediment .....	2—14
2.3.6	Sediment properties .....	2—17
2.3.7	Biological effects.....	2—18
2.3.8	Historical developments and human interventions.....	2—18
2.3.9	Dominant conditions .....	2—19
2.4	Conclusions and recommendations .....	2—20

---

<b>3</b>	<b>Small-scale sediment transport processes .....</b>	<b>3—1</b>
3.1	Flocculation .....	3—1
3.2	Settling and deposition .....	3—3
3.3	Sediment-fluid interaction .....	3—5
3.4	Self-weight consolidation .....	3—6
3.5	Erosion and entrainment.....	3—7
3.6	Sand-mud mixtures.....	3—9
3.7	Seasonal effects .....	3—11
3.8	Conclusions and recommendations .....	3—12
<b>4</b>	<b>Model requirements .....</b>	<b>4—1</b>
4.1	System-related requirements .....	4—1
4.2	Process-related requirements.....	4—2
4.3	Informatics-related requirements.....	4—4
4.4	Development phases.....	4—5
<b>5</b>	<b>Data requirements .....</b>	<b>5—1</b>
<b>A</b>	<b>Parameterisation of flocculation .....</b>	<b>A—1</b>

# I Introduction

## I.1 Background and objective of the study

The Sea Scheldt is the section of the Scheldt river between Ghent at the head of the Scheldt estuary and the Belgian-Dutch border near Doel<sup>1</sup>. A sub-section of the river between Rupelmonde (the limit of salt intrusion) and Doel is denoted as the Lower Sea Scheldt (Beneden Zeeschelde) and part of it forms the connection between the Port of Antwerp and the Western Scheldt. The Sea Scheldt and Western Scheldt form the Scheldt estuary.

The managing authorities, responsible for a proper functioning of the system, need to evaluate various measures that are anticipated in the nearby future to guarantee standards on safety, transport and water quality issues in the area. The fate of sediments in general, and of fine-grained cohesive sediments in particular, forms a crucial role in many of these managerial questions and the availability of a predictive tool in these matters is urgently requested.

This report describes necessary steps to set up a sediment transport model (or system of models) coupled to a numerical hydrodynamic model. The model is to be used to study questions related to the transport of cohesive sediment in the Lower Sea Scheldt and to assess siltation rates and sediment distribution in access channels. Furthermore, the effect of passive devices to reduce siltation rates and to modify sediment distribution needs to be quantified with the model.

## I.2 Set up of the study

To develop an adequate tool for cohesive sediment modelling the following aspects need to be considered:

- a. The model should be capable to address a number of existing urgent questions on cohesive sediment behaviour in the Lower Sea Scheldt. Some of these questions are described hereafter in Section 1.3 as examples;
- b. The model should be equipped with state-of-the-art process formulations regarding cohesive sediment dynamics;
- c. The model should be operated in a flexible and practical way, which poses requirements to architecture (e.g. coupling with other models and modules), runtime, user-friendliness and flexibility (e.g. the inclusion of new, more advanced process formulations).

These points stress the importance of a phased approach. It implies that on a short term (i.e. 2<sup>nd</sup> half of 2004) a dedicated model for the Lower Sea Scheldt should become available, employing process formulations in existing software, which is capable to address a number of current managerial issues. On the longer term, the cohesive sediment transport model

---

<sup>1</sup> *Upstream of Ghent, until its origin, the river is called Upper Scheldt (Bovenshelde).*

should be extended and improved with new insights, already partly available from literature but not yet implemented. In addition, future developments with respect to computational speed may allow for further detailed modelling of small-scale processes.

### 1.3 Managerial questions

The following ‘cases’ represent a number of managerial questions associated with the Lower Sea Scheldt. They are related to specific ‘engineering’ issues (e.g. siltation rates) as well as to more generic aspects on system behaviour (e.g. behaviour of turbidity maximum).

#### 1. *Dredging of the Zandvliet sill*

Formerly, the removed material from the Zandvliet sill consisted of sand, whereas presently mainly silt is being dredged. The reason for this change in composition of the dredged material is unclear, but possibly the construction of a container terminal nearby is related to this phenomenon. In addition, it should be investigated if continuous maintenance dredging is advisable as this may enhance local siltation rates.

#### 2. *Construction of the Oosterweel tunnel*

During the future construction of the Oosterweel tunnel the tunnel trench will gradually silt-up. Questions relate to aspects as (i) the location of the dump site of dredged material from the trench and (ii) dumping strategies to prevent recirculation.

#### 3. *Silting-up of tidal overflow areas*

Tidal overflow areas (‘Gecontroleerde OverstromingsGebieden’ or GOG’s) can be used to reduce high waters. The exact functioning of these areas needs further quantification, e.g. will they silt-up rapidly?

#### 4. *Effect of varying boundary conditions*

The effect of environmental conditions (seasonal varying river discharge and episodic events) on siltation rates and location needs further quantification.

#### 5. *Maintenance dredging of Deurganckdok*

The construction of the Deurganckdok required estimates on maintenance dredging quantities to evaluate the feasibility of the project. As part of an environmental impact assessment dumping on the Plaat van Doel will be considered to study the fate of the dumped material.

#### 6. *Composition of deposits in the Port of Antwerp*

The ratio of contaminated fluvial and relatively clean marine deposits in the harbours of Antwerp determines the (quality-based) classification of the dredged material. Mitigating measures may reduce this ratio resulting in more flexibility regarding dumping.

#### 7. *Ecological questions*

The impact of measures on the ecological functioning of the area is directly related to the transport of cohesive sediments and its effect on water quality. As such, a cohesive sediment transport model will play a key role in environmental impact studies.

The most urgent questions need to be resolved by the end of 2004. This largely determines the approach for the set up of a cohesive sediment transport model (what is possible?) in relation to the urgency of the managerial issues (what is needed?). This will be further discussed in Chapter 4 on model requirements.

## **1.4 Contents of this report**

In Chapter 2 a system description of the Lower Sea Scheldt is given, focusing on sediment characteristics, sediment sources, mud appearances, large-scale sediment transport processes. Also a historic overview of human interventions is presented. The underlying fundamental (small-scale) transport processes are described in detail in Chapter 3. The current state-of-the-art modelling is discussed as well as possible improvements of process formulations that are already available in literature. Both Chapters 2 and 3 result in requirements for the model to represent adequately the sediment dynamics in the Lower Sea Scheldt so that on the short term (by the end of 2004) managerial questions can be addressed. Further development of the model with improved process formulations will follow during subsequent years. This is elaborated in Chapter 4. Finally, Chapter 5 discusses the data requirements necessary for validation of the model.



## 2 Large-scale processes in the Lower Sea Scheldt

This chapter describes the physical processes in the Lower Sea Scheldt with emphasis on sediment dynamics. The objective is to highlight those processes that are considered to be essential for the transport of fine sediment in the Lower Sea Scheldt and consequently should be included in future, process-based, modelling tools. The emphasis in this chapter is on the large-scale characteristics of the Scheldt estuary, such as tidal asymmetry, gravitational circulation and channel-shoal interaction. Furthermore, data are described to supply future models with appropriate boundary conditions and for the calibration of these models. However, firstly topographical and geometrical features of the area will be discussed and the hydrodynamics as governed by the bathymetry, river discharge, the tide and the salinity-driven density currents will be summarised.

### 2.1 The Scheldt basin and Scheldt estuary

The Scheldt river originates in France near Gouy at an altitude of 100 m and debouches into the North Sea near Vlissingen at a distance of 350 km from its origin. The total catchment's area amounts 21,860 km<sup>2</sup> (de Schelde Atlas, 1999), see Figure 2.1. Between Ghent (160 km from Vlissingen) and the Belgian-Dutch border (60 km from Vlissingen) the river is denoted as Sea Scheldt while downstream of the border it is known as the Western Scheldt. The Sea Scheldt receives water from the Dender with its confluence at Dendermonde and the Rupel joining the Sea Scheldt at Rupelmonde. Downstream of Rupelmonde (100 km from Vlissingen) the river is called the Lower Sea Scheldt. Several tributaries merge to form the Rupel: the Dijle, the Zenne and the Demer (as tributaries of the Dijle) and the Beneden Nete, downstream of the confluence of the Grote and Kleine Nete.

The Scheldt estuary is defined as that part of the river basin with tidal influence. It consists of a fluvial estuary (or freshwater zone) between Ghent and Rupelmonde and a mixing zone between Rupelmonde and Vlissingen. The latter is subdivided into the upper estuary between Rupelmonde and the Belgian-Dutch border (Lower Sea Scheldt) and the lower estuary (Western Scheldt), see also Verlaan (1998).

The present Scheldt estuary is funnel-shaped with a total area of 370 km<sup>2</sup>. The width at the mouth of the estuary amounts to 6 km, 2-3 km near Bath and less than 100 m at Ghent. The average water depth of a cross-section decreases from 15 m near Vlissingen to 3 m at Ghent. The channels are deepest in the sharp bends (30-40 m).

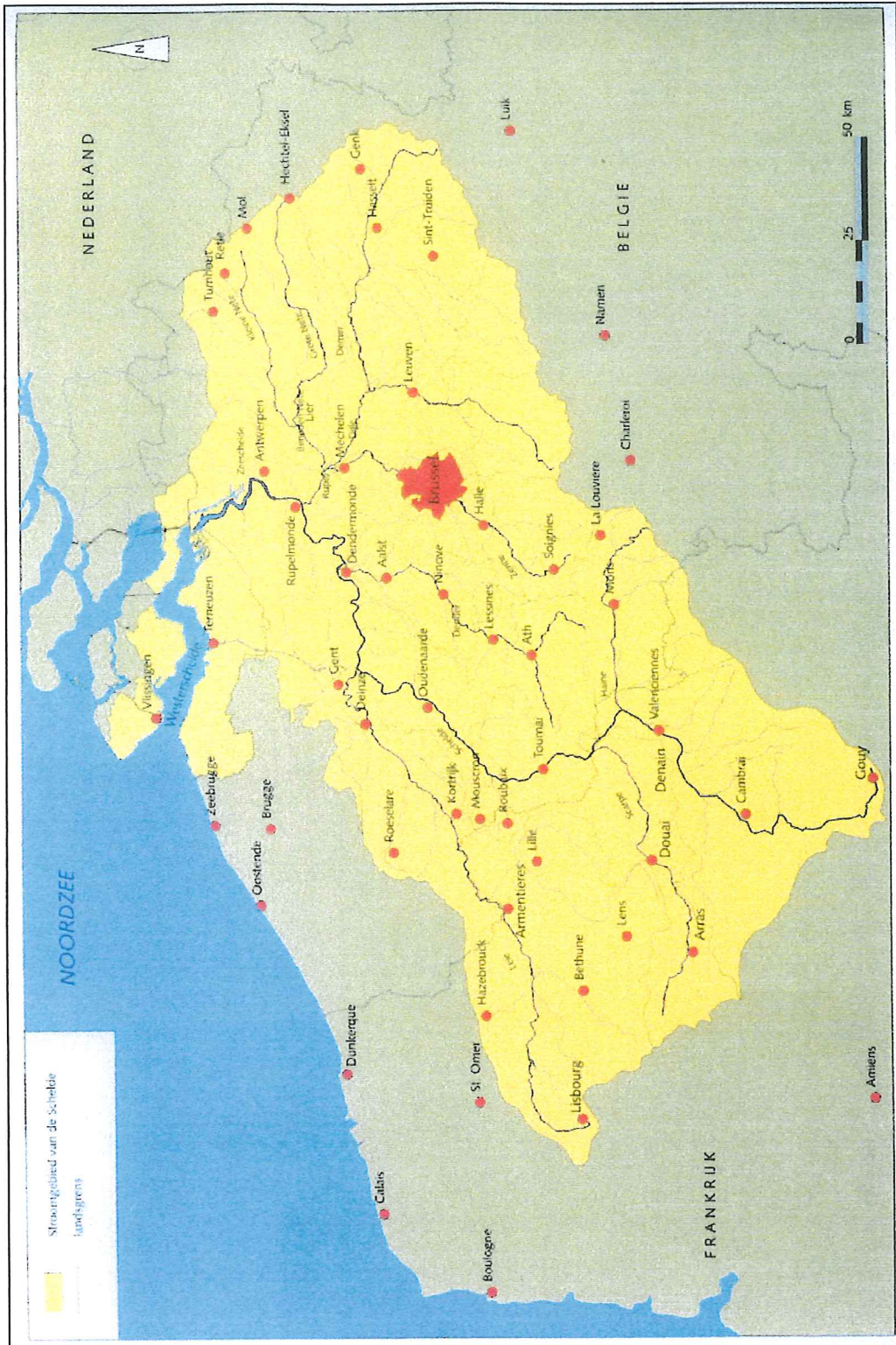


Figure 2.1: Catchment area of the Scheldt: topography (de Schelde Atlas, 1999).

## 2.2 Hydrodynamics

### 2.2.1 River discharge

The annual-averaged river discharge of the Scheldt river near Schelle, at the confluence of the Rupel and the Schelde, amounts to 110 m<sup>3</sup>/s with approximately equal contributions from the Rupel and the Schelde. However, variations from year to year can be large, ranging between 50 and 200 m<sup>3</sup>/s. Also seasonal fluctuations are significant with highest discharges (> 600 m<sup>3</sup>/s) between December and April.

Flow rates at various stations of the tributaries in the Scheldt catchment area are given in Table 2.1.

Tributary	Station	Flow rate [m <sup>3</sup> /s]
Upper Sea Scheldt	Melle (downstream Ghent)	22-31
Dender	Dendermonde	5-12
Zenne	Eppegem	9-12
Dijle (incl. Demer)	Haacht	25-27
Grote Nete	Itegem	4.5-6.5
Kleine Nete	Grobbendonk	5.5-7.5
Mouth of Rupel		55-65
Upper Sea Scheldt	Rupelmonde	45-55
Lower Sea Scheldt	Schelle	100-120
Lower Sea Scheldt	Belgian-Dutch border	100-140
Western Scheldt	Vlissingen	140-170

Table 2.1: Annual mean flow rates as measured during one or more years between 1970 and 1990 (Verlaan, 1998).

### 2.2.2 Vertical and horizontal tide

The tidal wave is mainly semi-diurnal with a mean tidal range of 3.8 m at Vlissingen, 5.2 m at Rupelmonde and 1.9 m at Ghent. The estuary can thus be classified as mesotidal to macrotidal. The effect of the spring-neap cycle is significant as follows from the amplitude ratio of the tidal constituents S<sub>2</sub> and M<sub>2</sub>: at Vlissingen 0.48/1.75 = 0.27 and at Antwerp 0.50/2.2 = 0.23. The propagating tide is blocked by weirs at Ghent and, in the Dender, near Dendermonde. In the lower reaches of the Dijle, Zenne and the Grote and Kleine Nete the tidal influence is still noticeable.

Average cross-sectional ebb and flood velocities are about 0.7 m/s. Maximum current velocities on the river are highest near Rupelmonde, 1.2 m/s during ebb and 1.4 m/s during

flood, and lowest near the Belgian-Dutch border. High water slack and low water slack occur approximately one hour after high and low water, respectively.

### 2.2.3 Tidal asymmetry

The ratio between the rise and fall time of the tidal wave decreases from 0.88 at Vlissingen to 0.75 at Rupelmonde and 0.39 at Ghent (Claessens and Belmans, 1984), indicating a strong asymmetry of the tide especially in the upper estuary. The interactions of the horizontal and vertical tide, and of the (semi-diurnal) tide with its overtides, generate net transport of sediment. In the case of flood-dominance, which is often the case in estuaries, tidal lagoons and tidal basins, the net transport of marine sediments is landwards and/or fluvial sediments are (partly) trapped within the system. Suspended sediment concentrations increase because (part of) the sediment is not deposited on the bed but remains in suspension.

A better representation of the tidal asymmetry can be obtained with the parameters  $a_4/a_2$  and  $2\phi_2 - \phi_4$  (ratio and differences of amplitudes and phases of the  $M_2$  and  $M_4$  tidal constituents). These can be compared with the morphological parameters  $a/h$  (ratio of the tidal amplitude and water depth) and  $V_s/V_c$ , (ratio of the storage volume and flow carrying volume), see Wang et al. (2002) and Winterwerp et al. (2002).

The tidal amplitude in Antwerp has increased by about 20% throughout the 20<sup>th</sup> century, while at Dendermonde an increase of almost 50% is observed. It is likely that the increase in tidal amplitude (and high waters) is caused by the large changes in the estuary, such as an increase in mean water level at Vlissingen, reclamations along the river, deepening and widening of the channels and channel alignments (Winterwerp et al., 2002).

### 2.2.4 Salinity intrusion

The tidal volume (= ebb + flood volume) is in the order of  $1.5 \cdot 10^9 \text{ m}^3$  near Vlissingen,  $0.2 \cdot 10^9 \text{ m}^3$  at the border and  $0.1 \cdot 10^9 \text{ m}^3$  at Antwerp (average values taken from Verlaan, 1998, and 'de Schelde Atlas', 1999). Based on the ratio of freshwater discharge and tidal volume, the estuary can be classified as partially mixed between Rupelmonde and Hansweert (only during high river discharges) and well-mixed downstream of Hansweert (Verlaan, 1998). However, the meandering of the river can cause lateral salinity differences giving rise to enhanced stratification, while also during slack water stratified conditions occur. Due to the river discharge the limit of salt intrusion can shift over a distance of 40 km, i.e. between Antwerp and 10-20 km upstream of Rupelmonde. On the Lower Sea Scheldt salinities vary between 0.5 and 10 ppt (Wartel and van Eck, 2000).

### 2.2.5 Gravitational circulation

Fresh water outflow in estuaries and lagoons generate longitudinal density gradients resulting in a vertical circulation in the system with a net landward near-bed current (gravitational circulation), causing a net flux of salt in upstream direction. If the estuary is well-mixed (due to tidal action and interaction with the bathymetry) the contribution of the gravitational circulation to the net up-estuary salt flux is relatively small. Verlaan (1998) concluded on the basis of the stratification-circulation diagram of Hansen and Rattray that

the up-estuary salt flux in the Scheldt estuary is mainly caused by diffusion and that gravitational circulation has only a minor contribution. This does not necessarily hold for the net flux of suspended sediment. As the near-bed suspended sediment concentration tends to be larger than the concentration higher in the water column, gravitational circulation will cause a net landward sediment transport.

## 2.3 Sediment dynamics

### 2.3.1 Input of fluvial/terrestrial sediment

Various studies have been carried out to quantify the input of fluvial (or terrestrial) fine sediment to the mixing zone of the Scheldt estuary (i.e. the area downstream of Rupelmonde). The results are summarised by Verlaan (1998) and presented hereafter.

According to Wollast and Marijns (1981) the total mud production in the Scheldt basin is  $753 \times 10^3$  ton/year. Distinction is made between mud of domestic, industrial and natural origin, see Table 2.2. The latter consists of erosion of muddy beds and agricultural effluent. The results from Wollast and Marijns were derived from a few transport measurements in a small part of the Scheldt catchment area during a period of one month only.

Sources	Mud production ( $\times 10^3$ ton/year) (Wollast and Marijns)	Mud production ( $\times 10^3$ ton/year) (IMDC)
Domestic	188	147
Industrial	294	68 - 104
Natural:	271	
• agriculture		4 - 34
• erosion		436 - 873
Atmospheric	-	1
<b>Total</b>	<b>753</b>	<b>656 - 1159</b>

Table 2.2: Sources of fluvial/terrestrial mud in the Scheldt estuary according to Wollast and Marijns (1981) and IMDC (1993).

Probably more reliable results are given by IMDC (1993) as they are based on much longer time series with a higher measurement frequency. In the IMDC study it was assumed that erosion of mainly loamy soils and mixed sand-loam soils occurs and that all eroded material consists of mud. Since up to 50% of these soils can contain sand, the quantity for natural mud erosion may be proportionally lower. This has also been indicated in Table 2.2. The main difference between both studies is that, according to Wollast and Marijns, the total terrestrial mud production consists of more or less equal contributions from domestic, industrial and natural sources. According to the IMDC study the contribution from natural sources (mainly erosion of muddy beds) is largest (~ 70%). No information on the inorganic and organic fraction of the various sediment sources has been found.

Part of the terrestrial mud will not reach the mixing zone due to deposition, dredging and decomposition processes. Besides, mud from the Leie basin (included in the quantities of Table 2.2) does not reach the Scheldt estuary, but is discharged directly to the North Sea (through the 'Afleidingskanaal van de Leie' and the 'Canal Ghent-Oostende') and the Western Scheldt (through the 'Gentse Ringvaart' and the 'Canal Gent-Terneuzen'). This results in the quantities of terrestrial mud, available for transport towards the mixing zone at Rupelmonde, as given in Table 2.3.

	Scheldt basin [10 <sup>3</sup> ton/year]	Rupel basin [10 <sup>3</sup> ton/year]	Mud entering the mixing zone [10 <sup>3</sup> ton/year]
Mud production	259 - 474	258 - 440	
Dredging amounts <sup>1)</sup>	254	156	
Available for transport	5 - 220	102 - 284	107 - 504

Table 2.3: Terrestrial mud production, dredging amounts and terrestrial mud available for transport (derived from Verlaan, 1998, and based on data from IMDC, 1993).

<sup>1)</sup> assuming a dry density of 450 kg/m<sup>3</sup>.

Direct measurements on suspended sediment concentration and river discharge were done at six locations: Schelde (Merelbeke), Dender (Dendermonde), Zenne (Epepegem), Dijle (Haacht), Grote Nete (Ipegem) and Kleine Nete (Grobendonk). Results are given in Figure 2.2, showing that between 1973 and 1986 the fluvial mud supply to the mixing zone varied between 300 10<sup>3</sup> and 800 10<sup>3</sup> ton/year with a mean of 390 10<sup>3</sup> ton/year (Verlaan, 1998).

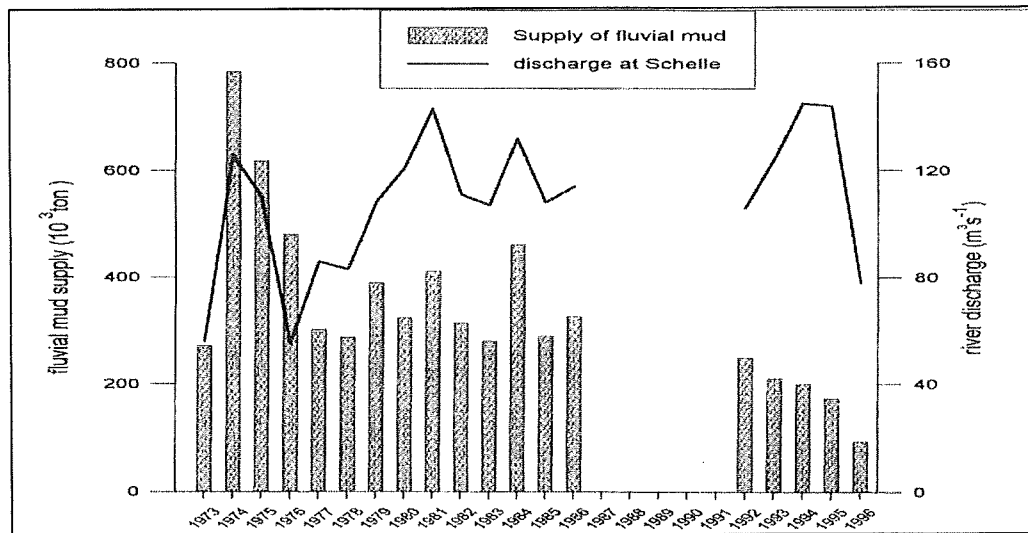


Figure 2.2: Annual fluvial mud supply to the Lower Sea Scheldt and annual mean river discharge (Verlaan, 1981).

The mean value is within the range as given in Table 2.3 (107 - 504 10<sup>3</sup> ton/year). Between 1992 and 1996 the fluvial input of mud appears to be lower, varying between 100 10<sup>3</sup> and

250  $10^3$  ton/year with a mean of 185  $10^3$  ton/year. During the latter period, measurements were done more frequently (weekly instead of monthly), allowing a better correction for peak discharges. The average fluvial mud supply for the whole period (1973-1986 and 1992-1996) amounts to  $340 \pm 160$   $10^3$  ton/year, which is in agreement with the result of Table 2.3 ( $300 \pm 200$   $10^3$  ton). It is also consistent with the fluvial sediment input at Schelle (downstream of the confluence of Rupel and Scheldt) reported by Van Maldegem (1993) (in: Wartel and van Eck, 2000), estimated at 400  $10^3$  ton/year.

According to Figure 2.2 a decreasing trend in the fluvial mud input can be observed since 1992. This also follows on a longer time scale by comparing the periods 1973-1986 ( $390$   $10^3$  ton/year) and 1992-1996 ( $185$   $10^3$  ton/year). This is attributed to the increased treatment of domestic waste water and the increased deposition upstream of Rupelmonde (due to the construction of a number of weirs and sluices) and the subsequent removal of fluvial mud (Verlaan, 1998). However, this decrease may also have (partly) been caused by a change in measuring methodology. Additional data for the latter period by Taverniers (2000), see Figure 2.3, show an increased mud input for the years 1998 and 1999, resulting in an average fluvial mud supply of  $200$   $10^3$  ton/year for the period 1992-1999 and an average of  $320$   $10^3$  ton/year for the combined period 1973-1986 and 1992-1999. The low (1996 and 1997) and high (1998 and 1999) input of fluvial sediment corresponds to low and high river discharges for these years (Wartel and van Eck, 2000).

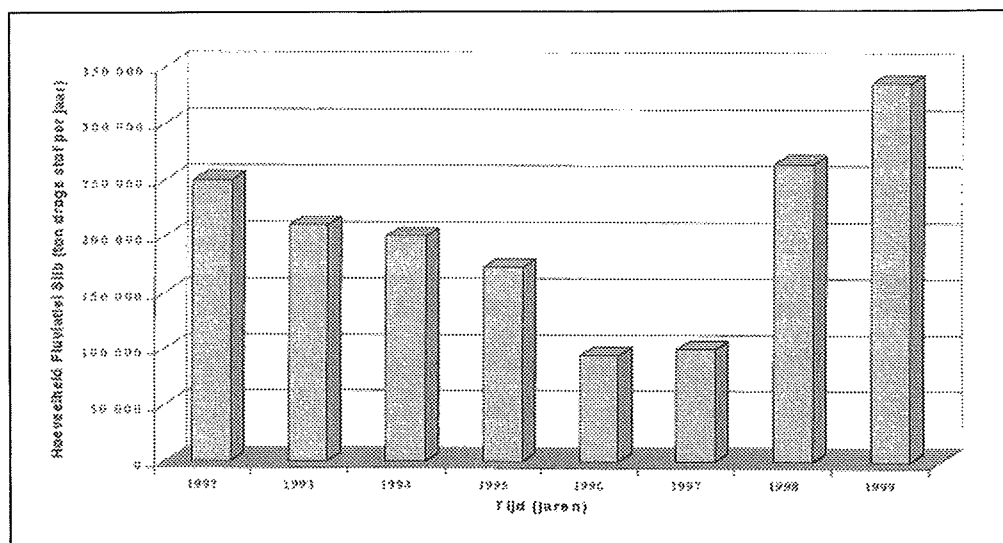


Figure 2.3: Annual fluvial mud supply to the Lower Sea Scheldt for the period 1992-1999 (Taverniers, 2000). From: Wartel and van Eck (2000).

The net fluvial sediment seaward transport at the border is estimated to be  $75$   $10^3$  to  $300$   $10^3$  ton/year, according to Salden and van Maldegem (1998) and van Maldegem (1993) (in: Wartel and van Eck, 2000).

Verlaan (1998) derived relationships between the suspended sediment concentration and river discharge at Rupelmonde for the years 1992-1993 and 1994-1995. Sediment transports at six locations at the edge of the estuarine zone were computed and added to obtain the total load at Rupelmonde. Concentrations were computed by dividing the total load to the river discharge at Rupelmonde. It appears that concentration increases with river discharge,

see Figure 2.4. However the correlation coefficients  $r^2$  are low: 0.28 and 0.65 for the two periods. Possibly better results can be obtained for the individual locations.

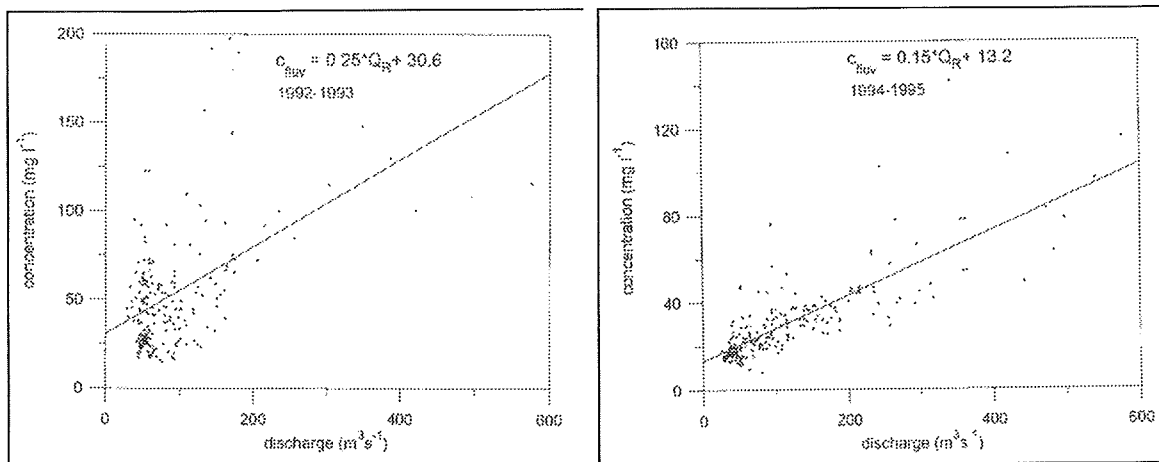


Figure 2.4: Concentration of fluvial suspended sediment versus river discharge at Rupelmonde for 1992-1993 (left panel) and 1994-1995 (right panel) (Verlaan, 1998).

The inventory of data on fluvial mud supply results in the following conclusions:

1. If no decreasing trend in the fluvial mud input to the mixing zone is assumed, the combined data for 1973-1986 and 1992-1999 result in a *long-term average fluvial mud supply* to the Lower Sea Scheldt of  $320 \cdot 10^3$  ton/year. Lowest and highest values for specific years are  $100 \cdot 10^3$  ton/year and  $800 \cdot 10^3$  ton/year, respectively.
2. Most recent data (1992-1999) show an average value of only  $200 \cdot 10^3$  ton/year with lowest and highest values for specific years of  $100 \cdot 10^3$  ton/year and  $330 \cdot 10^3$  ton/year.
3. The lower values for the period 1992-1999, as compared with the period 1973-1986, may be due to the increased measurement frequency or reflect an actual gradual decrease of fluvial mud input due to increased deposition and removal of fluvial mud in the Scheldt catchment area upstream of the mixing zone.
4. The major input of fluvial sediment is during periods with high river discharges.

It is recommended to establish relationships between the river discharge and suspended sediment concentrations for the tributaries upstream of Rupelmonde that contribute to the total fluvial sediment input of the Lower Sea Scheldt. Furthermore, the inorganic and organic fractions of the fluvial mud supply should be determined.

### 2.3.2 Input of marine sediment

Data on the input of marine sediment are much scarcer. Due to the continuous tidal fluctuation it is difficult, if not impossible, to derive reliable estimates for this quantity on the basis of measurements on flow velocities and suspended sediment concentrations. Mostly, the input of marine sediment follows as a closure term from a sediment mass balance. The input of marine sediment in the mouth of the Western Scheldt is estimated as  $130 \cdot 10^3$  ton/year of which most is deposited in the Western Scheldt itself (van Maldegem, 1993). However, depending on the assumptions for the mud balance the marine input may range between  $50 \cdot 10^3$  and  $300 \cdot 10^3$  ton/year. The input of marine sediment to the Lower Sea Scheldt, at the Belgian-Dutch border, is of course much less.



To check on the mutual consistency of the estimates for the fluvial and marine sediment input and the marine and fluvial fractions of the suspended sediment at the Belgian-Dutch border the various data are presented graphically in Figure 2.5:

- The average fluvial sediment transport at the Belgian-Dutch border is estimated as  $75 \cdot 10^3 - 300 \cdot 10^3$  ton/year (see Section 2.3.1).
- Given the fluvial sediment transport at the border  $T_{fluvial}$  the marine sediment transport at the border  $T_{marine}$  is related to  $p$  by:

$$T_{marine} = \frac{p}{100 - p} T_{fluvial} \quad (2.1)$$

where  $p$  is the marine fraction (%), varying between 20 and 60% (see Section 2.3.3).

- The enclosed area, as defined by Equ. (2.1),  $p = 20\%$  and  $p = 60\%$ , gives values for the marine sediment input at the border, which can be compared with other estimates (based on overall mud balances) of the input of marine sediment to the Lower Sea Scheldt.
- Estimates for the input of marine sediment at the mouth of the Western Scheldt amount to  $50 \cdot 10^3 - 300 \cdot 10^3$  ton/year and the input at the border much less (see above). This is written as:

$$T_{marine} = \alpha T_{marine}^{mouth} \quad (2.2)$$

where  $\alpha$  represents “much less” ( $\alpha \ll 1$ ). With  $\alpha = 0.2$  this results in the two horizontal lines in Figure 2.5 for the upper and lower estimates of the marine sediment transport in the mouth of the Western Scheldt.

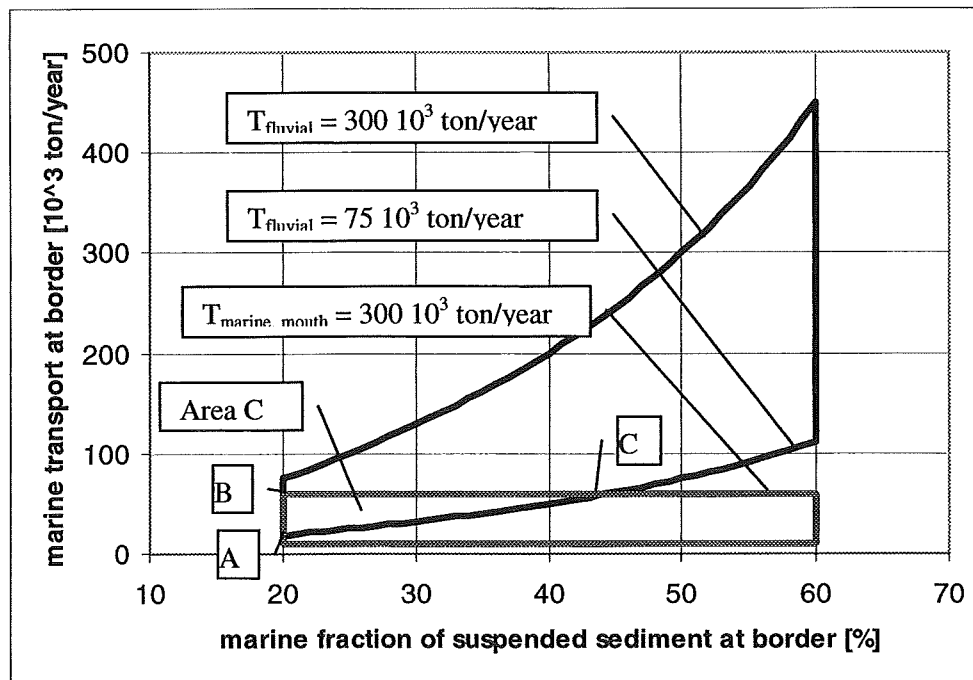


Figure 2.5: Ranges for fluvial and marine sediment transport at the Belgian-Dutch border.

From Figure 2.5 it follows that there is a relatively small area C for which all estimates are consistent. However, there are still many combinations of the individual quantities possible. This is illustrated by the derived values for the corner points of area C, see below (for  $\alpha = 0.2$ ). Note that point B (with a fluvial transport of  $240 \cdot 10^3$  ton/year at the border) implies that (almost no) sedimentation of fluvial sediment in the Lower Sea Scheldt would occur (the input of fluvial sediment at Rupelmonde is estimated as  $200 \cdot 10^3 - 300 \cdot 10^3$  ton/year). It is concluded that large uncertainties exist in the values for the various quantities.

$\alpha = 0.2$	Belgian-Dutch border		mouth Western Scheldt	
	$p$ [%]	$T_{marine}$ [ $10^3$ ton/year]	$T_{fluvial}$ [ $10^3$ ton/year]	$T_{marine}$ [ $10^3$ ton/year]
A	20	19	75	94
B	20	60	240	300
C	44	60	75	300

The analysis has implicitly assumed that the marine fraction of suspended sediment at the border is determined by the ratios of the fluvial and marine sediment transport at that location. However, if for some reason accumulation of marine sediment occurs, the curved lines will shift downwards (for a given  $T_{fluvial}$  less marine sediment is needed to arrive at the specified marine fraction of suspended sediment). Furthermore, only net sediment transports have been addressed.

Storm surges in the coastal zone will increase suspended sediment concentrations and enhance the import of marine sediments to the estuary. However, the time scale for the (net) transport is large so that the resuspended sediment originating from the North Sea may have settled before it reaches the Lower Sea Scheldt. Indeed, measurements at Prosperpolder during storm conditions did not indicate an increase of suspended sediment concentrations as compared with spring tide conditions and thus the direct effect of storm surges on sediment input to the Lower Sea Scheldt is probably small. However, storm surges do contribute to the overall availability of sediment in the system.

### 2.3.3 Mixing ratios of fluvial and marine sediments

Verlaan (1998) computed mixing ratios of fluvial and marine sediments (suspended and in the bed) for the Western Scheldt and the Lower Sea Scheldt by applying factor analysis to various data sets on chemical composition. The fraction of marine suspended sediment at the Dutch-Belgian border varies (more or less linearly) between 25% and 60% for river discharges between 200 and  $100 \text{ m}^3/\text{s}$ , see Figure 2.6.

Wartel and van Eck (2000) report values of 20 - 40% for the marine fraction (probably of suspended sediment) at the Belgian-Dutch border, as based on the composition of carbon isotopes. The estimates for the marine fraction in suspended matter thus range between 20 and 60%.

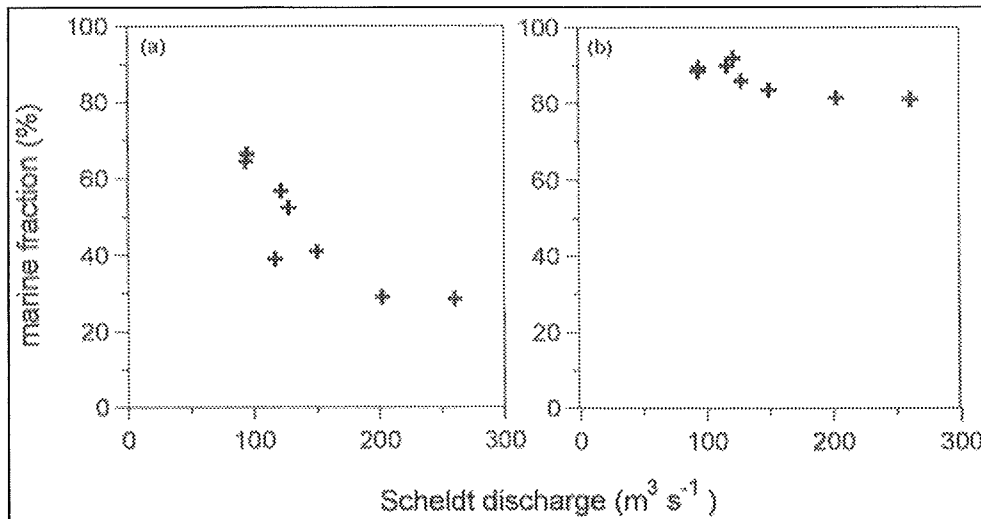


Figure 2.6: The fraction of marine suspended sediment versus the instantaneous Scheldt discharge at the Dutch-Belgian border (left panel) and Vlissingen (right panel) (Verlaan, 1998).

For the bed sediment it was found that in the upper estuary the marine fraction is less than 10%. Between Lillo (10 km upstream of the Belgian-Dutch border) and Saeftinge the marine fraction increases sharply from 10% to 70% (approximately 40 - 50% at the border), followed by a further increase in seaward direction, see Figure 2.7.

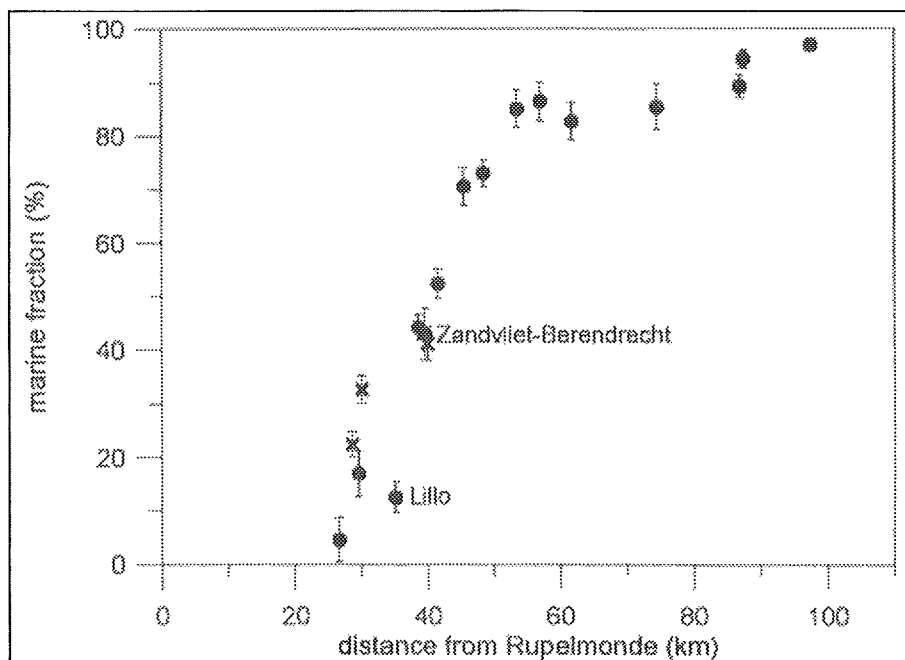


Figure 2.7: Fraction of marine bed sediment versus the distance from Rupelmonde (Verlaan, 1998).

●: samples taken from the main fairway

X: samples taken from the entrance channels to the harbour of Antwerp.

### 2.3.4 Bed sediment

The major internal source for the transport of sediment in the Lower Sea Scheldt is formed by the bed sediment. The dynamic exchange between the bed and the water column through

alternating erosion and deposition adds to the horizontal fluxes resulting from the input of marine and fluvial sediments at the boundaries of the Lower Sea Scheldt. An accurate representation of the actual locations and composition of bed sediments is important as it determines the spin-up time of future modelling tools. For instance: thick deposits on wrong places will result in spurious sediment transports for a period of time. This implies that sediment occurrences (location and thickness of deposits) and bed properties should be properly prescribed as initial conditions.

The bed of the Scheldt estuary consists of sand, mud and fluid mud. Upstream of Rupelmonde sediments consist of medium to coarse sands with a mud fraction ( $< 63 \mu\text{m}$ ) of less than 10%. Between Rupelmonde and Antwerpen, i.e. the area with maximum flow velocities, medium and coarse sands and locally gravel are found. Between Antwerpen and the Belgian-Dutch border bed sediments consist of sand, sandy muds and muds (Verlaan, 1998). The mud fraction on the bars of the navigation channel varies between 10% and 50%. In the entrance channels to the locks, especially the Kallo sluice, mainly fluid mud is found.

The lithography of the Lower Sea Scheldt, measured in 1999, is given in Figure 2.8. The upper meter of the bed consists of  $11 \cdot 10^6$  ton mud of which 25% in the access channels to the sluices (Wartel and van Eck, 2000). In the river, mud is mainly found in the inner bends, whereas sand and non-erodible beds are mostly present in the outer bends. Table 2.4 gives relative amounts of erodible mud for the various morphological entities in the Lower Sea Scheldt (and the Western Scheldt). The large amount of erodible mud in the channels is explained by the presence of the turbidity maximum in this part of the estuary (Wartel and van Eck, 2000).

<b>Morphological entity</b>	<b>Western Scheldt</b>	<b>Lower Sea Scheldt</b>
channels	20	61
intertidal (mudflats - 'platen')	10	0
intertidal areas (salt marshes - 'slikken')	25	26
salt marshes	25	7
shallow areas	10	0
harbours	10	6
<b>Total:</b>	<b>100</b>	<b>100</b>

*Table 2.4: Estimated relative amounts [%] of erodible mud of morphological entities (Wartel and van Eck, 2000).*

The large variability in sediment composition of course implies a large variability in sediment properties in general and in erodibility in particular. This is especially the case outside the turbidity maximum, such as the entire Western Scheldt.

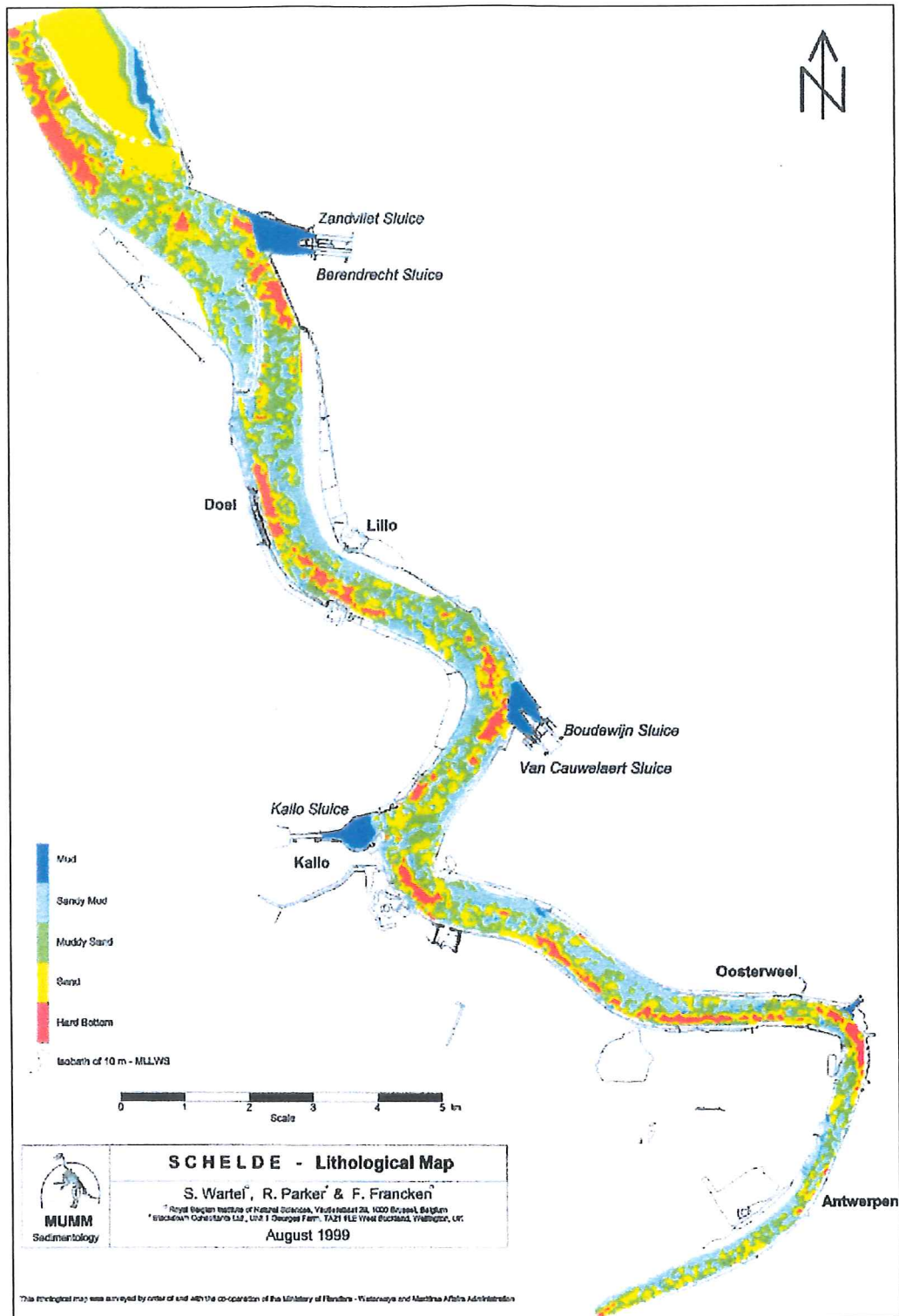


Figure 2.8: Lithography of the Lower Sea Scheldt (Wartel and van Eck, 2000).

Salt marshes, which inundate only during spring tides, can act as storage areas for mud. Sediment, which is not permanently stored on the salt marshes, may even accumulate for a period of 10 years. Furthermore, mud flats can act as temporary storage areas. Fettweis (1995) concluded that during summer periods the amount of mud stored on tidal flats is larger than during winter. This needs attention when selecting dominant/characteristic conditions for future simulations with numerical models. Average sand, mud and clay fractions (between Antwerpen and Zandvliet) for three types of deposits are given in Table 2.5.

Deposit	Sand fraction 2000-63 $\mu\text{m}$	Mud fraction < 63 $\mu\text{m}$	Clay fraction < 2 $\mu\text{m}$	Organic content
Stationary mud <sup>1)</sup>	4%	96%	59%	11%
Settled mud <sup>2)</sup>	30%	70%	42%	7%
Sandy	83%	17%	13%	2%

Table 2.5: Sand, mud and clay fractions and organic content of bed sediments in the Lower Sea Scheldt between Antwerpen and Zandvliet (Wartel and van Eck, 2000).

<sup>1)</sup> as present in the access channels (including fluid mud)

<sup>2)</sup> found in the river

Between Rupelmonde and Hoboken (near Antwerpen) the river bed cuts through the geological formation of Boom. This is a very cohesive clay deposit and thus highly erosion resistant.

### 2.3.5 Suspended sediment

The suspended sediment concentrations vary in time and space due to the non-steady hydrodynamics, the horizontal and the vertical circulations. These mechanisms cause a net landward transport of suspended sediment.

#### Tidal fluctuations

Suspended sediment concentrations may vary by a factor 2 to 10 with a good correlation with the varying tidal current (Verlaan, 1998). This suggests that on a small time scale the vertical sediment processes are dominant. Horizontal processes (circulations) become more important on a longer time scale. Generally, concentrations in the Lower Sea Scheldt are limited to several hundreds mg/l. Longitudinal suspended sediment concentrations, averaged for the period 1970-1990, are given in Figure 2.9.

Maximum and minimum values are for winter and summer conditions respectively. This difference is attributed to variations in river discharge (effect on turbidity maximum, sediment input), temperature (biological activity, flocculation etc.), storm effects (also on sea resulting in an increase of ambient suspended sediment concentrations) and changes in input from land erosion. Measurements further indicate that suspended sediment concentrations are larger during spring tide conditions than during neap tide conditions (Oosterweel and Prosperpolder).

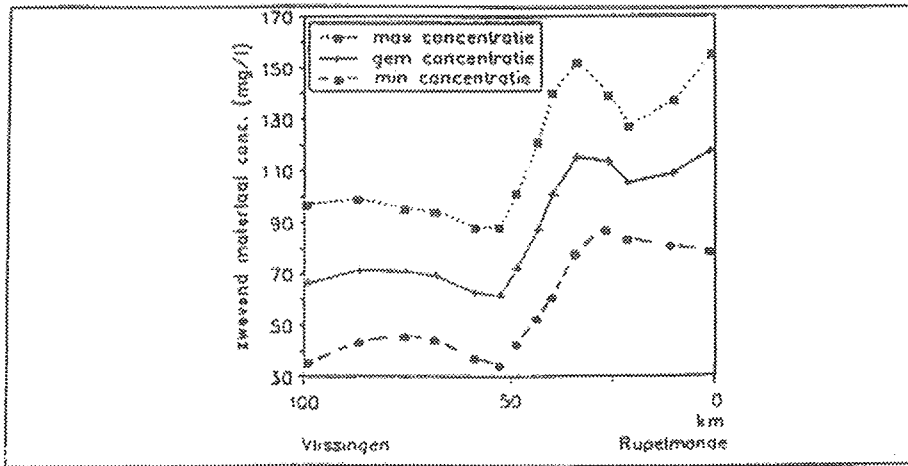


Figure 2.9: Longitudinal suspended sediment concentrations for the period 1970-1990 (van Eck et al., 1991).

### Turbidity maximum

The location of the turbidity maximum in estuaries is often related to the gravitational circulation, as sediment transport converges near the head of the salinity intrusion. When the suspended sediment profile is stratified, the landward transport will increase. This mechanism plays a role mainly in the (deeper) channels of the system, and is stronger for fine sediment with a larger grain size, as this sediment depicts a more pronounced vertical concentration gradient. In the Lower Sea Scheldt suspended sediment concentrations are highest between Antwerpen and the Belgian-Dutch border. The exact location of the turbidity maximum depends on the tidal phase and the river discharge, and their history. During periods with low river run-off the turbidity maximum is located upstream of Rupelmonde. Sometimes two turbidity maxima are found for discharges higher than 70 m<sup>3</sup>/s.

Other mechanisms responsible for the formation of turbidity maxima are tidal pumping (stemming from phase differences between water level, velocity and suspended sediment concentrations), asymmetry in the tide and bathymetry and salt water flocculation in relation to the hydro-sedimentological processes in the vertical. It is not known which of the mechanisms contributes most. This topic can be addressed by means of sensitivity analyses with future numerical models.

### Tidal asymmetry

According to current literature the asymmetry of the slack water periods during a tidal cycle is important for the transport of *fine-grained sediment suspensions*, more than the asymmetry of peak flood and ebb current and period. This asymmetry is the result of overtides, present in the external tidal forcing of the system and/or generated within the system by non-linear interactions. Landward transport (i.e. flood dominance) prevails if  $(dU/dt)_{HWS} < (dU/dt)_{LWS}$ , where  $U$  is a characteristic (depth-averaged) flow velocity component and HWS and LWS stand for high water slack and low water slack respectively. This mechanism generates net transports only in conjunction with the lag effects mentioned hereafter. For *coarser sediment* (sand), the tidal asymmetry in the peak velocities becomes

important, in particular the ratio of the amplitude of the vertical tide of the  $M_2$  and  $M_4$  overtide and their phase difference  $2\phi_{M_2} - \phi_{M_4}$ . If the phase difference (of the vertical tide) is positive, the transport in the estuary is flood-dominated. It can be reasoned contrary to the current literature, that for fine-grained sediments the asymmetry in slack period and peak velocities may **both** be important, depending on the sedimentological status of a particular system (Winterwerp, 2003).

### Lag effects

Two so-called lag effects determine the net transport of suspended sediments; its direction is governed by asymmetry effects (and possibly gravitational circulation) as discussed above:

- *Settling lag*: Around slack water, when the flow is no longer able to keep sediment in suspension, the sediment will settle. However, settling takes time, as a result of which the sediment is transported beyond the point where the flow falls below its transport capacity. Hence, sediment settling velocity and (local) water depth governs the magnitude of settling lag.
- *Scour lag*: Following slack water, the flow accelerates and will re-erode the sediment deposited during slack water. However, flow velocities (bed shear strength) to re-erode sediment deposits are larger in general than the flow velocity to keep the sediment in suspension. Hence, bed strength, erosion rate and vertical mixing time govern the magnitude of scour lag.

These effects can be summarised with the observation that less energy is required to keep fine cohesive sediment in suspension than to bring it in suspension.

### Temperature and flocculation effects

As many basins are much shallower than the surrounding sea, their water temperature is expected to be larger in summertime and lower in wintertime. As a result, temperature density currents may occur. Moreover, the settling velocity of the sediment will alter throughout the season because of temperature-induced variations in viscosity ( $\mu_{T=6C} = 1.45 \text{ mPa}\cdot\text{s}$  and  $\mu_{T=16C} = 1.10 \text{ mPa}\cdot\text{s}$ , i.e. a increase in settling velocity by 25 %). It is not known whether this effect plays a role in the Scheldt estuary.

The settling velocity of cohesive sediment flocs may also vary (largely) as a result of flocculation processes. This is in particular the case in and around the turbidity maximum of estuaries.

### Channel-shoal interactions

Estuaries, tidal lagoons and inlets are often characterised by large longitudinal gross ebb (export) and flood (import) transports of fine sediment, in particular in their mouth. If part of the sediments entering the system during flood is deposited on intertidal areas, a net import of fine sediment is the result. This is a very effective trapping mechanism, governed by the small-scale channel-shoal exchange processes, which was concluded from an analysis of data of the "Friesche Zeegat", a tidal inlet in the Dutch Wadden Sea.



## Water level effects

The *mean* water depth in systems with pronounced intertidal areas is smaller during high water slack (HWS) than during low water slack (LWS), as a result of which a larger fraction of sediment will settle during HWS than at LWS. Moreover, during HWS, the shallow parts, situated near the head of the system, are flooded. Hence, the landward transport during flood is not, or only partly balanced by a seaward transport during ebb. The magnitude of the net landward transport is determined by the bathymetry of the system and the lag-effects discussed above. Interaction of these mechanisms often results in flood-dominated transport over the intertidal areas and ebb-dominated transport in the estuary channel.

## Wave effects

Waves stir up sediment deposits and/or prevent the sediment from settling. The wave activity in shallow areas like intertidal flats is often so large, that net sedimentation of fine grained sediments on these flats seems impossible. Indeed, many flats in estuaries, lagoons and inlets are mainly sandy. However, many muddy intertidal flats are frequently encountered as well, and such mudflats play an important role in the overall mud balance of estuaries, lagoons and inlets. The physical processes governing the sediment dynamics on mudflats are not sufficiently understood at present.

## High-concentration suspensions

Near the bed, layers with much higher concentrations, ranging between 1 and 100 g/l, can be present (denoted by Wartel and van Eck, 2000, as stationary mud). They are formed during slack water and resuspended during the subsequent phase of the tide when flow velocities increase. Parts of the high-concentration layer may survive, especially during neap tide conditions. In that case the layer will consolidate resulting in a net accumulation of sediment (settled mud) and thus inducing a net transport over a neap-spring cycle. Stationary mud (or fluid mud) layers are mainly found in the entrance channels to the locks of the Port of Antwerpen (especially the Kallio lock). It is also found on the intertidal areas along the salt marshes and behind artificial structures for shore protection. In the river mud layers are found only occasionally (Wartel and van Eck, 2000).

### 2.3.6 Sediment properties

The anorganic fraction of suspended sediment of the Lower Sea Scheldt consists of quartz and clay minerals. The latter is mainly represented by illite, see Table 2.6. The sand fraction in the bed can contain relatively large amounts of glauconite.

Mineral	Lower Sea Scheldt	Western Scheldt
Illite	37	34
Vermiculite	13	-
Chlorite	11	6
Smectite	23	49
Kaolinite	16	11

Table 2.6: Clay minerals [%] in the Lower Sea Scheldt and Western Scheldt (Wartel and van Eck, 2000).

The stationary mud (in the access channels to the sluices) and the settled mud (on the river bed) contains large amounts of carbonates. In the suspended material the carbonate content increases in downstream direction due to increased mixing with sea water.

The organic content of the suspended material is larger than that of the bed material (see also Table 2.5). It varies with the river discharge and is further affected by phytoplankton bloom.

### 2.3.7 Biological effects

A number of biological effects can be distinguished with their typical seasonal cycle:

- fixation by micro-phytobenthos and bacteria, in particular from early spring to early summer, sometimes with a second peak in late summer,
- pelletisation by filter feeders; these organisms filter the sediment from the water column at a large rate and pelletise the mineral components of the sediment, increasing their effective settling velocity by a few orders of magnitude,
- burial: a number of organisms bury fine-grained sediments during their activities.

Such effects are for instance observed during spring season in the Dollard estuary, The Netherlands, when sediment deposits are stabilised by biological activity, as a result of which the overall turbidity in the system decreases substantially.

### 2.3.8 Historical developments and human interventions

The morphology and bathymetry of the Scheldt estuary has changed significantly over the last millennium as a result of natural processes and human interventions. Throughout the centuries up till the nineteen seventies the tidal volume has decreased, e.g. due to the reclamation of Braakman (1952) and Sloe (1960). The total water surface has decreased from 50,000 hectares (500 km<sup>2</sup>) in 1800 to 35,000 hectares (350 km<sup>2</sup>) for the present situation. An overview of historical developments and human interventions is given in Table 2.7, see also Winterwerp et al. (2002).

19 <sup>th</sup> & 20 <sup>th</sup> century	Land reclamation, dike construction and channel rectification	<ul style="list-style-type: none"> <li>• 1877-1908: nine bends between Ghent and Durme mouth</li> <li>• 1902-1904: Scheldt bend upstream of Durme</li> <li>• After 1930: bend rectification on the Durme</li> <li>• 1955: dam construction on the Durme at Lokeren.</li> </ul>
1960's	Loss of appr. 5000 ha of wetlands between Lillo and Bath	Remaining wetlands: Groot Buitenschor (11 ha), Galgenschor (45 ha), Schorren van Ossendrecht, Waarde en Bath (75 ha).
	Loss of polders at both sides of the Scheldt due to extension of Port of Antwerp.	Six polders such as: <ul style="list-style-type: none"> <li>• Polder 'Pijp Tabak': 7000 ha, left bank Zwijndrecht.</li> <li>• Polder Berendrecht: 8000 ha right bank.</li> </ul>
1955-1996	Western Scheldt: <ul style="list-style-type: none"> <li>• Western part: net erosion of 20 10<sup>6</sup> m<sup>3</sup></li> <li>• Central part: net deposition of 30 10<sup>6</sup> m<sup>3</sup></li> <li>• Eastern part: net erosion of 60 10<sup>6</sup> m<sup>3</sup></li> </ul>	Large-scale channel deepening and maintenance dredging through the bars in the main ebb channel in the eastern part. Dumping in the estuary outside the maritime access routes.
1977-present	Flood protection measures (Sigma plan): modifications of dikes (level and strengthening) and construction of controlled flood areas.	<ul style="list-style-type: none"> <li>• Controlled flood areas ('Gecontroleerde Overstromingsgebieden' or GOG's): 533 ha.</li> <li>• Only flooding several times per year during storm conditions.</li> </ul>
1997-1998	General deepening programme (48/43 ft) of maritime access routes.	
On-going	Sand mining in the Western Scheldt and Lower Sea Scheldt for public construction works: 3.5 Mton of sand per year.	
Present-coming years	Construction of Kruikeke-Bazel-Rupelmonde controlled flood area. Further deepening of the fairway.	<ul style="list-style-type: none"> <li>• With reduced tidal regime: "Gecontroleerd Gereduceerd Getijdegebied" or GGG: 600 ha</li> <li>• Flooded during each tide.</li> </ul>

Table 2.7: Historical (and planned) developments and human interventions in the Scheldt estuary (derived from Winterwerp et al., 2002)

The human interventions may have caused the observed increase of the tidal amplitude in the Scheldt estuary, thus responsible for large-scale morphological changes. It is likely that the system is still responding to the human interventions as listed in Table 2.7.

### 2.3.9 Dominant conditions

As described in the previous sections, the sediment dynamics in the Lower Sea Scheldt is governed by a large number of external factors, associated with variations of the tide, river

discharge, meteorology, biology and human interventions. The question is what conditions govern the physics that are relevant for the managerial issue (see Section 1.3) under consideration and how these conditions are addressed by the models. Some general thoughts are given hereafter.

Suspended sediment concentrations and related sediment fluxes are higher during spring tide than during neap tide due to the larger flow velocities and erosion rates. During neap tides the vertical exchange of sediment between the bed and the overlying water column will be less and consolidation of the accumulated sediments on the bed may occur. Because the hydrodynamics and sediment dynamics for spring and neap tides show a distinct behaviour it may be necessary to consider full neap-spring tide conditions. Also the locations of maximum deposition at the turbidity maximum will vary during the 14.5 days neap-spring cycle, because of the varying effects of tidal pumping and gravitational circulation. Flocculation processes may determine the local sedimentation rates. Furthermore, the larger tidal range during spring tide allows the sediment to be stored (temporarily) on tidal flats (flooding each tide) and salt marshes (only flooding during spring tide). Simulations over a 12.5 hrs period with specific tidal amplitudes may show to what extent the sediment dynamics during a 14.5 days period can be reproduced.

Seasonal variations result from the varying input of fluvial and marine sediments. During periods with high river run-off sediment input is largest; mixing curves of suspended and bed sediment indicate that sedimentation of suspended matter mainly occurs under high discharge conditions. In addition the location of the turbidity maximum and the magnitude of the estuarine circulation is affected. Wind affects the sediment dynamics, especially on the mud flats, also with a seasonal component. The consequences of rainfall on the properties of mud on tidal flats is yet unknown. Biological influence on the sediment properties (i.e. the organic content, algae mats) is related to the bloom of phytoplankton, reflecting changes on a seasonal time scale.

Episodic events, such as storms, can have an impact on the input of marine sediments. The extent to which this affects the sediment dynamics in the Lower Sea Scheldt is not clearly understood yet, but it is probably not large on small time scales.

## 2.4 Conclusions and recommendations

The large scale behaviour and transport processes of fine cohesive sediment in the Beneden Zeeschelde (Lower Sea Scheldt) are characterised as follows:

1. The sediment consists of a mixture of marine and fluvial contributions. Around Antwerp, the marine fraction of bed sediments amounts to about 40 – 50 %. The input of fluvial sediment into the system is reasonably well known, whereas the marine input is poorly known.
2. Also from a granular point of view the sediment is mixed. For instance, the sand-mud composition varies widely over the Scheldt estuary, yielding large variations in sediment properties (erodibility).
3. The suspended sediment concentration varies largely with mean maxima up to a few 100 mg/l, where higher values are observed in winter time and correlate with spring tide and high river flow.

4. Fine marine and fluvial sediments are trapped in the Scheldt estuary in general, and in the turbidity maximum around Antwerp in particular. This trapping is the result of bathymetrical effects, tidal asymmetry, gravitational circulation and channel shoal interactions. In the latter case, biological effects play a major role.
5. Meteorological and biological effects and variations in river flow generate important seasonal variations in suspended sediment concentrations and sediment supply.

These observations imply the following strategy in developing a numerical fine sediment transport model for the Lower Sea Scheldt:

- It is concluded that, initially, full neap-spring tide simulations with a high river discharge are needed to account for the major sediment transport characteristics of the Lower Sea Scheldt. The applicability of shorter simulations with a cyclic (semi-diurnal) tide and constant river flow should be assessed, together with the effects of seasonal variations.
- It is recommended to further analyse the relative importance of the large-scale processes: tide and tidal asymmetry, river discharge, gravitational circulation (density effect due to salinity differences), amount and ratio of fluvial and marine sediment input, lag effects (as influenced by the sediment properties), etc.
- Simulations in the form of sensitivity studies will have to show the importance of seasonal variations, episodic events, biological effects, etc.
- Attention should be paid to the time scales of the large-scale processes. The residence time of river water in the Scheldt estuary is approximately 3 months, and for mud much longer due to alternating deposition and erosion. These time scales will have repercussions for the duration of numerical simulations (spinning-up of the model).
- It is further recommended to establish relationships between the river discharge and suspended sediment concentrations for the tributaries upstream of Rupelmonde that contribute to the total fluvial sediment input of the Lower Sea Scheldt. In addition, the inorganic and organic fractions of the fluvial mud supply should be determined.

The approach, as described above, will isolate the dominant large-scale processes in the estuarine system of the Lower Sea Scheldt. This is important as it determines how the cohesive sediment transport models will be applied to answer the specific managerial questions.

## 3 Small-scale sediment transport processes

The transport cycle of cohesive sediment is governed by a number of key processes:

- flocculation, i.e. the formation and break-up of flocs of cohesive sediment,
- settling and deposition of cohesive sediment, including the effect of hindered settling,
- interaction between suspended cohesive sediment and turbulent flow at high suspended sediment concentration, such as in the case of fluid mud formation,
- consolidation, in particular self-weight consolidation, including the effects of minor amounts of fine sand,
- erosion and entrainment of fresh and consolidated deposits,
- sand-mud mixtures.

This chapter briefly presents descriptions of each of these processes, giving attention to common modelling approaches and their limitations as well as to more advanced modelling techniques. However, literature is overwhelming and a full treatment is not possible within the scope of this report. The major part of the text in the subsequent sections is derived from the book *Cohesive Sediment in the Marine Environment* by J.C. Winterwerp and W.G.M. van Kesteren, which is currently under preparation.

In addition, a number of topics may need attention as they affect (the modelling of) the cohesive sediment transport cycle:

- non-Newtonian behaviour of sediment-water mixtures, i.e. the stress-strain relations when soft mud deposits show a liquid behaviour,
- the effect of navigation,
- biological effects (bio-stabilisation and –destabilisation),

There are not yet state-of-the-art formulations to take the last three processes into account in sediment transport modelling and therefore they are not discussed in this report. It is recommended to further investigate the relative importance of these processes.

### 3.1 Flocculation

Flocculation is the result of mutual collisions of, and subsequent adherence between particles of cohesive sediment, and break-up is caused by turbulent stresses and mutual collisions. The effects of the latter are small for cohesive sediment. The flocculation process is governed by three agents:

- Brownian motion cause the particles to collide and form aggregates,
- Particles with a large settling velocity will overtake those with a smaller settling velocity: collisions between these particles may result in aggregation (generally referred to as differential settling), and
- Turbulent motion will cause particles, carried by turbulent eddies, to collide and form flocs; turbulent shear on the other hand may disrupt the flocs, causing floc break-up (generally referred to as shear effects).

Mathematical-physical formulations for the collision frequency by the three agents mentioned above are well known and are given in many papers and reviews. From these, it can be concluded that aggregation due to Brownian motion and hindered settling is probably small in estuarine and coastal environments. Measurements on the effect of turbulence reveal that the mean floc size first increases with shear rate, followed by a decrease, and that the floc size increases with increasing suspended sediment concentration. The shear rate is a measure of the turbulent shear of the flow and follows from:

$$G = \sqrt{\frac{\varepsilon}{\nu}} \quad (3.1)$$

in which  $\varepsilon$  is the turbulent dissipation rate per unit mass and  $\nu$  is the kinematic viscosity of the suspension. It can be obtained from a turbulence model or from the relationship:

$$\varepsilon \approx \frac{u_*^3}{\kappa h} \frac{1 - \zeta}{\zeta} \quad (3.2)$$

where  $u_*$  is the shear velocity,  $\kappa$  the Von Kármán constant, and  $\zeta = z/h$  the relative elevation above the bed. The particle diameter is then computed from the following heuristic formula:

$$D_f = D_r \frac{1 + aG}{1 + bG^2} \quad (3.3)$$

where  $D_f$  and  $D_r$  are the floc diameter and reference diameter respectively and  $a$  and  $b$  are empirical coefficients. Formula (3.1) was applied by Malcherek (1995) with a three-dimensional model in a numerical study on the suspended sediment concentrations in the Weser estuary. That author reported that he was able to simulate the observations properly only when using this formulation.

From a review of available literature it follows that many studies have been carried out on the effects of turbulence on the flocculation process. Some of these studies are rather descriptive, others more fundamental, and some entirely empirical. They all describe the variation in the number of particles or estimate the maximum floc size that can be achieved. Only occasionally the important variation in floc size and settling velocity with time is described.

Winterwerp (1998, 2002) developed a flocculation model, which employs functions for the aggregation and break-up of mud flocs due to turbulent shear stresses. It assumes that the aggregation due to Brownian motion and hindered settling and the break-up due to interparticle collisions are of minor importance. Two model parameters, a flocculation parameter and a floc break-up parameter, have to be determined empirically, e.g. by using data from laboratory or field measurements. The model allows the computation of the equilibrium and maximal attainable floc size and settling velocity, the maximal values being smaller than the equilibrium values due to the limited residence time of flocs in the water column. Functional relationships for the maximal floc size and settling velocity are derived

in Appendix A. Currently, coefficients are being determined at the University of Plymouth utilising a data base on floc properties. Furthermore, fluid mud concentrations can be predicted with the model.

Presently, the model formulations have been implemented in a one-dimensional vertical numerical model. With this point model flocculation dynamics can be simulated at specific locations, neglecting advection and assuming constant sediment concentration (Lagrangian approach). The results, specifically the settling velocity of mud flocs and concentrations of fluid mud layers, can then be used as input for a large-scale cohesive sediment transport model. A full coupling of a three-dimensional sediment transport model and an advanced flocculation model is currently not possible because of excessive computing time. However, the implementation of a parameterised form of the flocculation processes, such as described in Appendix A, is feasible and probably necessary in the turbidity maximum.

### 3.2 Settling and deposition

Flocculation of cohesive sediment, as discussed in Section 3.1, results in an increase of the settling velocity of the suspended sediment. As the environmental conditions may vary, e.g. during a tidal cycle, a neap-spring cycle and on a seasonal time scale, the settling velocity cannot be considered as a constant. Although progress is being made on the prediction of the settling velocity as a function of hydrodynamic conditions and physico-chemical properties of the fluid and the sediment, a rigorous treatment is still incomplete. It necessitates the performance of in-situ field measurements on the settling behaviour of mud flocs. These measurements may focus either on the assessment of the settling velocity itself or on the floc diameter. In the latter case the settling velocity *of single flocs in still water* (thus at low volumetric concentrations) is derived from the following expression, which is based on a large number of field data:

$$w_{s,r} = \frac{\alpha}{18\beta} \frac{(\rho_s - \rho_w)g}{\mu} D_p^{3-n_f} \frac{D_f^{n_f-1}}{1+0.15Re_f^{0.687}} \quad (3.4)$$

Where  $w_{s,r}$  is the settling velocity of a single mud floc in still water,  $\alpha$  and  $\beta$  are coefficients depending on the shape (sphericity) of the particles,  $\rho_w$  and  $\rho_s$  are the densities of the water and the sediment (primary particles),  $\mu$  is the dynamic viscosity of the water,  $D_p$  and  $D_f$  are the diameters of the primary particles and the flocs and  $Re_f = w_{s,r} D_f / \nu$  which is the particle Reynolds number with  $\nu$  as the kinematic viscosity. The power  $n_f$  represents the fractal dimension of the flocs, which varies between 1.7 and 2.3 for estuarine conditions with an average of 2.0. In the latter case the settling velocity is proportional to the floc diameter. Equ. (3.4) is valid for floc diameters up to a few 100  $\mu\text{m}$ .

At high volumetric concentrations the flocs start to hinder each other due to several processes (e.g. return flow, particle-particle collisions and interactions, reduced gravity, cloud formation), resulting in a decrease of the settling velocity. This effective settling velocity is commonly described with a modification of the semi-empirical Richardson-Zaki formula:



$$w_s = w_{s,r} (1 - k\phi_f)^n \quad (3.5)$$

where  $w_s$  is now the reduced settling velocity due to hindered settling,  $\phi_f$  is the floc volume concentration,  $k \approx 1$  and  $n$  is a function of the particle Reynolds number:  $2.5 < n < 5.5$ .

A probably more realistic approach is given by Winterwerp (2002), where a mud as well as a sand fraction is considered. In the case of only mud the hindered settling formula reads:

$$w_s^m = \frac{(1 - \phi_f)(1 - \phi_s)}{1 + 2.5\phi_f} w_{s,r} \quad (3.6)$$

where  $\phi_f$  and  $\phi_s$  are the volume concentrations of the mud flocs and the primary particles respectively:  $\phi_f = c / c_{gel}$ ,  $\phi_s = c / \rho_s$ ; the gelling concentration (i.e. fluid mud concentration)  $c_{gel}$  is computed with the flocculation model or is obtained from measurements. The hindered settling regime is bounded by  $\phi_f < 1$ ; for  $\phi_f \geq 1$  we are in the consolidation regime.

The deposition rate is commonly expressed by Krone's formula:

$$\frac{dh\bar{c}}{dt} = -D = -w_s c_b \left( 1 - \frac{\tau_b}{\tau_d} \right) \quad \text{for } \tau_b < \tau_d \quad (3.7)$$

where  $D$  is the deposition rate,  $\bar{c}$  is the depth-averaged concentration,  $c_b$  is the near-bed concentration (often  $c_b$  is set equal to  $\bar{c}$ ),  $\tau_b$  the bed shear stress and  $\tau_d$  the so-called critical shear stress for deposition. Equ. (3.7) is often used in conjunction with an erosion formula employing a critical erosion shear stress which is usually larger than the critical shear stress for deposition. In that case either deposition or erosion occurs. However, this approach cannot explain many laboratory experiments on deposition and erosion and is also not capable to simulate observed sediment dynamics in the field. This is discussed by Winterwerp and van Kesteren (2004) and an alternative approach is proposed. This approach is based on the following assumptions: (i) erosion and deposition take place simultaneously, (ii) the erosion rate employs a critical shear stress for erosion which is time dependent because of physico-chemical processes (consolidation, gelling and restructuring), (iii) the bed shear stress is given by a probability density function reflecting the turbulent fluctuations near the bed and (iv) at low concentrations flocculation is mainly determined by the near-bed turbulent flow, and flocculation over the water depth or with time does not play an important role.

At high concentrations flocculation is important and deposition results in the formation of fluid mud, which is governed by other processes. With these assumptions the classical deposition tests by Krone could be reasonably simulated. It led to the conclusion that at low concentrations the deposition flux is given by  $W_s c_b$ . The increase of the critical shear stress for erosion can be obtained from a consolidation model when evolution in time is important

(e.g. during a neap-spring cycle or in case of seasonal effects). Due to uncertainties in the critical shear stress for erosion, the bed shear stress and the erosion parameter (which scales the erosion flux) it is not recommended to apply the probability function for the bed shear stress.

### 3.3 Sediment-fluid interaction

The properties of sediment-laden flow in the marine environment may be highly affected by the sediment carried by this flow. As a result a pronounced interaction between the (turbulent) flow field and the suspended sediment exists. This is not only the case under rare and exotic conditions: such interactions are common in sediment-laden open channel flow. It will be assumed hereafter that the sediment-water mixture can be considered as a one-phase fluid in which all particles follow turbulence movements, except for their settling velocity. This is a valid approximation if  $w_s \ll u_*$ , where  $u_*$  is the shear velocity. Sediment-fluid interactions comprises a number of effects (Winterwerp and van Kesteren, 2004):

- Hydraulic roughness as induced by bed-forms, which are the result of an interaction between the sediment transport and the hydrodynamics. This has been extensively described in literature for non-cohesive sediments; for cohesive sediments (or mixtures of cohesive and non-cohesive sediments) the present knowledge is still very limited as no systematic studies have been performed.
- Turbulent structure of the flow field as affected by the bed properties (permeability of sand beds and visco-elastic or visco-plastic behaviour of cohesive beds). Most of the present knowledge is related to the turbulent flow over rigid, impermeable walls.
- Erodibility as influenced by inflowing and outflowing pore water.
- Increased apparent viscosity due to the presence of sediment particles
- Increased bulk density of the single-phase fluid due to the presence of suspended sediment.
- Damping due to vertical gradients of the fluid density (buoyancy effect).
- Drag reduction due to flow laden with cohesive sediment (clay).
- Other effect such as reduction of the Reynolds number due to an increase of the viscosity, gas-related effects and non-linear behaviour of cohesive sediment

From literature it follows that (non-cohesive) sediment in suspension has an effect on the vertical velocity distribution of the flow and on the vertical diffusivity. This has been attributed to buoyancy effects, i.e. the damping of turbulence by the suspended sediment, often described through a reduction of the Von Kármán constant with increasing concentration. Also stratification effects have been considered and the eddy viscosity was reduced as a function of the local Richardson number. Though still no conclusive explanation exists as experimental evidence is sometimes contradictory, sediment-induced buoyancy effects appear to play an important role. This has been illustrated by Winterwerp (2001) using 1DV simulations to predict the velocity profile for the cases without and with suspended sand particles taking into account a sediment-induced buoyancy term. The model was able to simulate experimental data for both cases. It was concluded (Winterwerp and van Kesteren, 2004) that the entire velocity profile in sediment-laden flows is affected by sediment-induced buoyancy effects. This is reflected in changes both in the logarithmic part and in the core region of the turbulent flow (defect law). These changes are properly predicted with computations with the standard  $k-\varepsilon$  turbulence model, including a sediment-induced buoyancy destruction term and a constant Von Kármán constant  $\kappa_s$ , i.e. the value for

buoyant-neutral conditions. These buoyancy effects have major implications for the behaviour of cohesive sediment suspensions, in particular at high concentrations. Under saturated conditions a total collapse of the concentration profile may even occur, resulting in the formation of fluid mud.

This was demonstrated by Winterwerp and van Kessel (2002) who applied a three-dimensional model to (i) a schematic case representing a coastal area with a tidal river, navigation channel and harbour basin and (ii) the Rotterdam harbour area. The model included hindered settling, buoyancy destruction in the turbulence  $k$ - $\epsilon$  model, accounting for turbulence damping of vertical density gradients, and sediment-induced baroclinic pressure gradients (i.e. due to density differences) in the momentum equations. It appeared that the sediment transport into the harbour area increased by a factor 3 to 5 and that this large effect stems from steeper vertical gradients of suspended sediment concentrations. These results were already obtained at moderate concentrations ( $\approx 100$  mg/l); at higher concentrations the increase will be much larger. In an estuary rapid siltation due to sediment-induced buoyancy effects (and flocculation) may occur around slack water.

A High-Concentration Mud Suspension (HCMS) is defined as a sediment suspension for which the flow field is measurably affected by sediment-induced buoyancy effects, but still exhibits Newtonian properties. These suspensions, with concentrations of several 100 to a few 1,000 mg/l, have been observed frequently. Most observers found large interactions of the suspension with the flow field, and significant drag reduction has been reported.

### 3.4 Self-weight consolidation

Layers of soft mud, that have accumulated on the bed as a result of deposition, show a gradually decrease in water content. Water is squeezed out from the pores (and mud flocs) due to the self-weight of the mud, resulting in a gradual decrease of the layer thickness. It is accompanied by large deformations, due to the high initial water content and the resulting low stiffness of the grain skeleton. A mathematical description of this process is given by the Gibson equation, which employs the mud properties in the form of two functions: (i) the effective stress as a function of the void ratio and (ii) the permeability as a function of the void ratio. This implies that history effects, channelling and formation and break-up of flocs are not included. It can be shown that the Gibson equation is also valid for the settling phase when no effective stresses have yet developed.

When the material functions are known the Gibson equation can adequately describe the process of self-weight consolidation. However, small variations in material functions yield large differences in consolidation behaviour which makes the results uncertain. The material functions are often described in terms of power laws using four or five coefficients. The actual values of these coefficients depend on grain size distribution (clay content), organic content, activity and pore size distribution. The scatter can be large and consequently laboratory tests are needed to assess the precise values.

Assuming a fractal structure of the bed it is possible to derive material functions for the consolidation equation of sediment-water mixtures. These functions also have the form of power law relations. It can be shown that the various parameters can be determined from observations of the evolution of the interface and from the final density profile, i.e. no

permeability or stress measurements have to be carried out. If a relation between the sediment strength and effective stress is used, it is possible to set-up an integrated model to simulate (hindered) settling, consolidation and re-entrainment. The fractal dimension, describing the structure of the bed, is much larger than the values typical for flocs in the water column. This must be due to the squeezing of the flocs in the bed under self-weight consolidation. However, physical-mathematical descriptions describing this transition in floc structure are not available at present. This implies that integrated settling-consolidation-erosion models require input of two structural parameters, i.e. two values of the fractal dimension  $n_f$ .

Numerical solution of the consolidation equation requires a detailed vertical discretisation and small time step to obtain accurate results. Yet, the settling-consolidation-erosion sequence described above is representative only for a short period in the long-term transport and fate of cohesive sediment in the natural environment. However, a complete integration of the settling and consolidation models in full three-dimensional sediment transport models is not feasible at present from a computational time point of view, in particular when the bed level is increasing, c.q. decreasing by continuous deposition and erosion. An approximate solution to the consolidation equation, which is less time-consuming, is available and has been implemented and tested in Delft3D software. For thin consolidating layers deformations are small and the consolidation equation can be made linear. This results in a diffusion equation for the excess pore water pressure for which a solution can be found efficiently. The method allows long-term computations at acceptable computational effort of the bed development, when the total amount of sediments varies over time as a result of sedimentation and/or erosion. Note that this approach has been developed for homogeneous sediment mixtures only, i.e. segregation of sand and mud should not occur. However, a small sand fraction may be included in the consolidating sediment layer.

### 3.5 Erosion and entrainment

The transport and fate of cohesive sediment in the marine environment is governed to a large extent by water-bed exchange processes, i.e. deposition and erosion. The erosion rate of deposits, as a function of the local hydrodynamic conditions (flow and waves), may vary by orders of magnitude, depending on the sediment-pore water composition and properties, degree of consolidation, stress history, etc. Moreover, often only thin layers of a few mm to a few cm of the bed are eroded in one tidal cycle. Yet, when mixed over the water column, the eroded sediment may increase the local suspended sediment concentration by many ten to hundred mg/l, depending on the local water depth. Within such thin layers, large gradients in physico-chemical properties may occur, affecting the erodibility of the sediment. This explains, amongst other things, why the literature contains so many different erosion formulae with a large range in parameter values. Various modes of erosion can be distinguished, depending on the bed properties, such as strength and permeability, and the stresses applied by the water movement: entrainment, floc erosion, surface erosion and mass erosion.

*Entrainment* occurs when the mud is so soft that it behaves as a viscous fluid. This may be the case when deposits are formed by rapid siltation, for instance forming fluid mud in a navigational channel, or by liquefaction of mud deposits by wave action. When the upper layer is turbulent and the mud layer not, as in the case of stationary fluid mud, the mud is

entrained by the water column (Case I). In that case the sediment-water interface will lower. If the mud layer is turbulent, as in the case of a turbidity current, water from the upper layer is entrained by the mud layer, resulting in a rise of the sediment-water interface (Case II). Laboratory Case I experiments can be properly simulated with a one-dimensional vertical model with a numerical model with a standard  $k-\varepsilon$  turbulence model, taking into account the effects of buoyancy destruction and hindered settling. Explicit formulations exist and have been tested and implemented. For Case II entrainment the standard  $k-\varepsilon$  turbulence model is not very accurate. If both layers are turbulent, turbulent mixing between the two layers may occur.

*Floc erosion* is referred to when (a part of the) flocs at the bed surface are disrupted individually by the water movement. This may occur when the flow-induced (peak) bed shear stresses exceed the strength of the floc or the adhesion of the floc to the rest of the bed. Floc strength and adhesion may decrease in time by cyclic stresses by the turbulent flow field and/or wave action. Floc erosion rates are not large by its nature of individual floc rupture. However, it is a very continuous process and may contribute to the overall erosion rate considerably. At present, this erosion process is poorly understood.

*Surface erosion* can be regarded as a drained failure process. Continuity requires that sediment particles, removed from the bed surface, are to be replaced by water. This implies that flow of environmental water into, or of pore water within the bed is an important process. The top of the bed liquefies as a result of swell when the bed is over consolidated, and/or as a result of hydrodynamic pressure fluctuations, induced by the turbulent flow field and/or waves. In literature various (empirical) formulations can be found that describe surface erosion. In a generalised form the erosion rate  $E$  can be given by:

$$E = M F \left( \frac{\tau_b - \tau_e(z, t)}{\tau_e(z, t)} \right) S(\tau_b - \tau_e) \quad (3.8)$$

where  $M$  is a scaling factor,  $F$  is an excess shear stress function (e.g.  $F(X) = X^n$ , and  $S(x)$  a ramp function:  $S = 0$  for  $x < 0$ , and  $S = 1$  for  $x > 0$ ). Note that  $\tau_e$  may also decrease in time because of swell, liquefaction and other processes when the sediment is subjected to turbulent shear or wave induced stresses. The critical shear stress depends on parameters as the dry density of the bed, the plasticity index, the mud content and mud properties (mineralogy as reflected by the CEC) and pore water properties (SAR). However, prediction of the critical bed shear stress (and the erosion scaling parameter  $M$ ) on the basis of these parameters is still not possible. Laboratory tests may supply the necessary data to derive the proper input parameters for the erosion rate expression, but flume experiments tests are expensive and do not (always) represent in-situ conditions. Alternatively, the erosion parameters may follow from calibration of the sediment transport model against field data.

A new approach, where erosion is considered as a drained process, has resulted in an erosion function, which employs parameters that can be assessed relatively easy by means of simple laboratory tests (e.g. Winterwerp and van Kesteren, 2004):

$$E = \frac{c_v \rho_d}{10D_{50} (1 + W_{cr} \rho_s / \rho_w)} \frac{\tau_b - \tau_{cr}}{c_u} \quad (3.9)$$

where  $c_v$  is the consolidation coefficient,  $\rho_d$  is the bed dry density,  $D_{50}$  is the median size of the primary particles,  $W_{cr}$  is the water content at the critical state,  $c_u$  is the undrained shear strength and  $\tau_{cr}$  is the critical shear strength. The latter is related to the Plasticity Index ( $PI$ ) according to:

$$\tau_{cr} = 0.163 PI^{0.84} \quad (3.10)$$

Note that  $c_u$  and  $\rho_d$  vary with depth, but that all other parameters are constant when the sediment composition does not change. This formula is very similar to Equ. (3.8), describing the surface erosion as a drained process.

*Mass erosion* can be regarded as an undrained failure process. In this case, external flow-induced stresses exceed the undrained shear strength of the bed, and lumps of material are removed. This mode of erosion occurs in particular in the case of turbulent flow or waves over irregular beds. Cliff erosion (e.g. on intertidal mudflats) is a well-known form of mass erosion. This mode of erosion is poorly understood at present. Experiments suggest that mass erosion can occur when:

$$\frac{1}{2} \rho U^2 > (2 \text{ to } 5) c_u \quad (3.11)$$

where  $c_u$  is the undrained shear strength (remoulded shear strength). Because of the stochastic behaviour of mass erosion, no erosion rate expression can be given.

Waves may cause three forms of failure: surface erosion, mass erosion and massive liquefaction. The latter is the result of cyclic loading of the bed by wave-induced stresses. The liquefied layer may become subject to entrainment processes or develop into a turbidity current. Modelling of the liquefaction process requires advanced numerical tools. A coupling with two- or three-dimensional hydrodynamic and sediment transport models is not yet feasible because of the required computing resources. The application of a one-dimensional vertical model seems more appropriate to study under what conditions liquefaction may occur. In the case of surface erosion wave-induced bed shear stresses exceed flow-induced bed shear stresses easily by an order of magnitude. Moreover, as a result of non-linear effects, the net bed shear stress induced by waves and currents is larger than their arithmetic sum.

### 3.6 Sand-mud mixtures

Sediment occurrences in natural environments are commonly mixtures of non-cohesive and cohesive fractions. The addition of clay and/or silt (if sufficiently large) will affect the sand skeleton as described by the maximum and minimum porosity. The maximum porosity may

be used as a discriminator between sand-skeleton dominated or clay-skeleton dominated sediment, and between sand-skeleton dominated or silt-skeleton dominated, i.e. whether the sand grains are able to form a skeleton or not. The next step in classifying in-situ cohesive sediments is combining the discriminators for sand- or silt-dominated skeletons with the cohesive behaviour of the clay-water system. This can be done with the sand-silt-clay triangle to classify soils based on the basis of grain size distribution in combination with in-situ density or in-situ porosity. The various discriminators divide the sediment triangle in six sub-zones, distinguishing six modes of sediment behaviour:

1. non-cohesive sediment dominated by sand skeleton,
2. cohesive sediment dominated by sand skeleton,
3. non-cohesive sediment with unstable skeleton,
4. cohesive sediment dominated by clay skeleton,
5. non-cohesive sediment dominated by silt skeleton, and
6. cohesive sediment dominated by silt skeleton

Thus the general sand-silt-clay triangle can be reduced to a site-specific diagram if the in-situ porosity  $n$  or dry bed density  $\rho_{dry}$  is known. This results in the  $\xi^{sa} - \rho_{dry}$  diagram of Figure 3.1 that is constructed for Western Scheldt sediments as an example. It can be regarded as a phase-diagram for bed behaviour in natural environments.

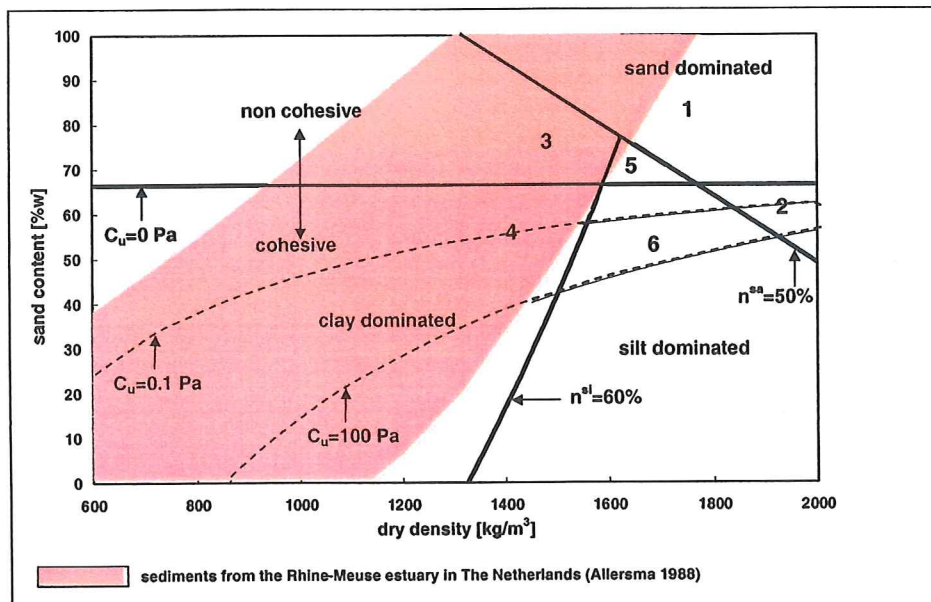


Figure 3.1: Sediment-phase diagram for Western Scheldt sediments (Winterwerp and van Kesteren, 2004).

The shaded area is enclosed by upper and lower bounds for the dry density as expected in nature. From Figure 3.1 it can be deduced that three modes of sediment behaviour are expected to be encountered in the Western Scheldt:

- mode 1: non-cohesive sand dominated behaviour,
- mode 3: non-cohesive very loose (sensitive to liquefaction) sand/silt skeleton, and
- mode 4: cohesive clay dominated behaviour.

The classification, as described above, is useful to select appropriate erosion functions for the various types of beds as encountered in nature. It was applied by van Ledden (2003) in

modelling the erosion behaviour of sand-mud beds. Process formulations based on Equ. (3.8) were implemented in Delft3D and applied to schematic cases as well as a natural system (Friesche Zeegat). The effect of (small amounts of) sand can also be included in hindered settling formulations for mud as well as in the material functions for consolidation, describing the compressibility and permeability of sand-clay beds.

### 3.7 Seasonal effects

Physical and biological seasonal effects can be distinguished:

#### 1. Physical seasonal effects

The seasonal variability of the wind and wave conditions should play an important role, as large areas with deposits of fine-grained sediment can be eroded under storm conditions: it has been suggested for instance that the Wadden Sea exports fine-grained sediments during storm conditions. However, significant wave effects on intertidal areas occur already at moderate wind conditions (Beaufort 4 to 5), prevailing almost throughout the year. Another seasonal effect concerns temperature fluctuations: an increase in temperature lowers the fluid viscosity, hence augments the sediment settling velocity.

#### 2. Biological effects

A number of biological effects can be distinguished with their typical seasonal cycle:

- fixation by micro-phytobenthos and bacteria, in particular from mid spring to mid summer, sometimes with a second peak in autumn,
- pelletisation by filter feeders; these organisms filter the sediment from the water column at a large rate and pelletise the mineral components of the sediment, increase their effective settling velocity by a few orders of magnitude,
- burial: a number of organisms bury fine-grained sediments during their activities,
- destabilisation by digging and locomotion.

These biological effects are summarised nicely in a diagram by Widdows and Brinsley (2002), shown in Figure 3.2.

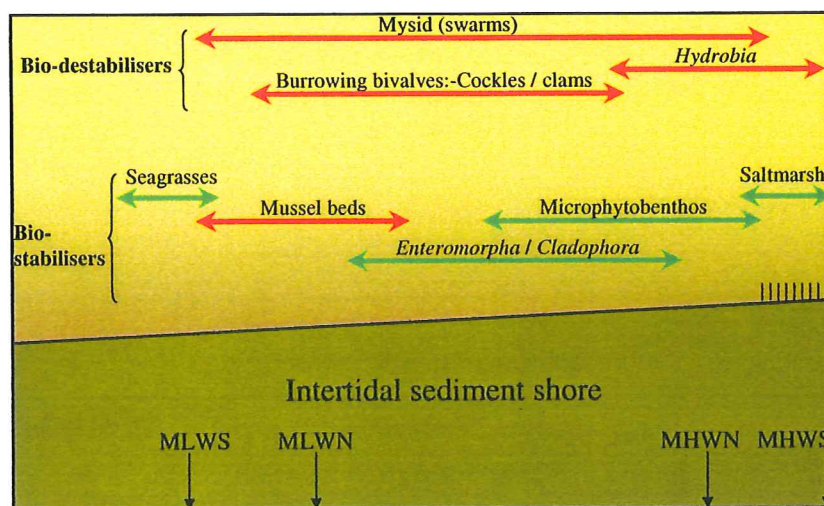


Figure 3.2: Classification scheme of biological effects on intertidal sediment dynamics (Widdows and Brinsley, 2002).



Such effects are for instance observed during spring season in the Dollard estuary, The Netherlands, when sediment deposits are stabilised by biological activity, as a result of which the overall turbidity in the system decreases substantially (van der Ham, 1999, de Brouwer, 2002).

### 3.8 Conclusions and recommendations

In this chapter a number of small scale processes have been identified that govern the fine sediment dynamics in the Beneden Zeeschelde. In particular the following processes have been addressed:

1. water-bed exchange processes in general and in particular erosion of the bed and its consolidation. This is one of the key factors in a calibrated numerical model.
2. the influence of biology on the physical processes in general and on their seasonal variations in particular.
3. the influence of flocculation on the sediment's settling velocity, in particular in the turbidity maximum.
4. the effect of sediment composition (sand-mud ratio) on the water-bed exchange processes. This plays especially a role in the turbidity maximum of the Beneden Zeeschelde.

Sections 3.1 through 3.7 have presented summaries of the various process formulations as part of the sediment transport cycle. Distinction has been made between presently available formulations and more advanced modelling approaches. It is recommended to investigate the potentials and limitations of new approaches step by step:

- The application of formulations for *deposition and erosion*. Sensitivity runs, as described in Section 2.4, should be performed and the effect of simultaneous deposition and erosion investigated (see Section 3.2).
- The inclusion of *sediment-fluid interaction* as this may largely affect the transport of suspended sediment.
- The role of *flocculation* can be simulated with the 1DV point model. Simulations for the access channels will show the conditions that govern the development of fluid mud layers. Parameterised formulations for flocculation can be incorporated in three-dimensional transport model(s).
- The effect of neap-spring cycles on *consolidation and erosion*. The parameterised consolidation model (see Section 3.4) can be applied as part of the Delft3d software package. The effect on the shear strength of the bed during a neap-spring tidal cycle should be investigated.
- The *entrainment of fluid mud* layers due to tidal flow.
- The role of *biology*. This needs to be further studied to determine the relative importance in relation to the other processes and to assess seasonal effects.
- The effect of *waves*.

## 4 Model requirements

### 4.1 System-related requirements

#### Spatial scales and sub-areas

Due to the density driven flow, resulting from salinity differences between river and sea water, salinities and suspended sediment concentrations in the Lower Sea Scheldt can vary strongly in horizontal and vertical direction. The degree of stratification varies during the semi-diurnal tidal cycle as well as during the neap-spring tidal cycle and is affected by the river discharge. A depth-averaged approach is suitable if stratification of salinity and suspended sediment concentration profiles is small, but in other cases a three-dimensional model is preferable to simulate sediment transports.

Upstream of the limit of salt intrusion (i.e. on the Sea Scheldt and Scheldt river including tributaries) the necessity of a three-dimensional model is less and a depth-averaged approach can be followed.

Downstream of the lower boundary of the Lower Sea Scheldt processes are also three-dimensional due to fresh water – salt water interaction. Modelling of this area (i.e. the Western Scheldt including the coastal area) with a 3D-model will require a large computing effort. Moreover, the additional value of such a model over a depth-averaged approach is limited, because also many other processes such as channel-shoal interaction, horizontal circulations and biological influences affect sediment transports. Proper modelling of these processes are currently still under investigation and as such a depth-averaged model for the Western Scheldt is more appropriate. However, such a model should account for sediment mixtures in general, and for the role of sand-mud mixtures in particular as this affects the large scale transport considerably.

The application of a depth-averaged model for the whole area, i.e. Western Scheldt and coastal area, Lower Sea Scheldt and upper reaches of the Scheldt river until the tidal limit, will allow the derivation of boundaries conditions for the Lower Sea Scheldt.

#### Time scales

Processes vary on time scales of the semi-diurnal tide, the neap-spring tidal cycle and during the various seasons. The model should be capable addressing all these time scales depending on the questions to be solved. To limit computation time, long-term simulations (over the seasons) for a large area (Western Scheldt) can best be performed with a two-dimensional model. Three-dimensional simulations are feasible provided that the modelled area is not too large (e.g. Lower Sea Scheldt).

The system-related requirements are summarised as follows:

Area	Type of model	Function
Western Scheldt incl. coastal area (Voordelta), Lower Sea Scheldt and upper reaches of the Scheldt river.	Two-dimensional, depth-averaged (2Dh)	<ul style="list-style-type: none"> <li>• Boundary conditions for 2Dh and 3D model of the Lower Sea Scheldt</li> <li>• Large-scale simulations</li> <li>• Sediment balance</li> <li>• Variations in boundary conditions</li> <li>• Simulations on all relevant time scales (up to seasons)</li> </ul>
Lower Sea Scheldt <sup>1)</sup>	Two-dimensional, depth-averaged (2Dh)	<ul style="list-style-type: none"> <li>• Approximate simulations, esp. for well-mixed conditions</li> <li>• Pilot simulations for 3D-model</li> <li>• Simulations on all relevant time scales (up to seasons)</li> </ul>
Lower Sea Scheldt <sup>1)</sup>	Three-dimensional (3D)	<ul style="list-style-type: none"> <li>• Detailed simulations</li> <li>• Simulations on all relevant time scales (up to seasons)</li> </ul>

<sup>1)</sup> The lower and upper boundaries of the model will be Waarde and Schelle respectively.

## 4.2 Process-related requirements

The need to answer practical questions on a relatively short term (end of 2004) requires that firstly existing models should be employed. Although these models have their limitations in describing the physical processes in detail, as indicated in Chapter 3, they can significantly contribute in answering the aforementioned questions. Confidence in the predictive capabilities of the model will be enhanced by a thorough validation, which stresses the importance of data acquisition by means of field measurements (see Chapter 5). Further possible improvements of the descriptions of the physical processes are already available, partly from literature and partly in research versions of models, but it will take time to implement and test in operational software. Consequently, distinction is made to the set-up of:

- (i) a state-of-the-art model during Phase 1, which includes available and already implemented process formulations on cohesive sediment transport and,

(ii) the set-up of an advanced model during Phase 2, which includes available process formulations not yet implemented.

This distinction between the two successive phases is only applicable to the three-dimensional model for the Lower Sea Scheldt.

The process-related requirements *for the 3D model* of the Lower Sea Scheldt are given in the table below.

Processes:	State-of-the-art model	Advanced model
<b>flocculation</b>	functional dependency on salinity and suspended sediment concentration	to be assessed
<i>settling &amp; hindered settling</i>	functional dependency on suspended sediment concentration	to be assessed
<i>sediment-fluid interaction</i>	explicitly modelled	explicitly modelled
<b>sediment-induced gravity currents regarding HCMS</b>	explicitly modelled	explicitly modelled
<b>sediment-induced gravity currents regarding Fluid Mud</b>	explicitly modelled	explicitly modelled
<i>sedimentation and siltation</i>	<ul style="list-style-type: none"> <li>• explicitly modelled</li> <li>• computation of bed accumulation</li> </ul>	to be assessed
<b>consolidation</b>	explicitly modelled	to be assessed
<b>erosion and re-entrainment</b>	<ul style="list-style-type: none"> <li>• explicitly modelled with 'Partheniades' approach; now available as a single empirical function</li> <li>• computation of bed erosion</li> </ul>	to be assessed
<i>bed boundary conditions and rheology</i>	<ul style="list-style-type: none"> <li>• bed density and strength specified</li> <li>• no rheological modelling</li> </ul>	to be assessed
effect navigation	not modelled	to be assessed
<b>sand-mud mixtures</b>	not modelled	modelling of sand and mud fractions incl. bed module
biological effects	not modelled	to be assessed
morphology	not modelled	not modelled

Processes printed in *italic* have been described and implemented in the software, processes printed in **bold** have been described and tested in a different software environment; for the other processes no tested formulations are available at present. Note that it is implicitly assumed, that a calibrated 2Dh and/or 3D hydrodynamic model, covering the relevant domain(s), is available.

### **4.3 Informatics-related requirements**

Three software packages are considered to simulate the transport of cohesive sediment:

1. DELFT3D (developed by WL | Delft Hydraulics),
2. WAQUA, c.q. TRIWAQ (developed by Rijkswaterstaat of the Ministry of Transport and Public Works of The Netherlands) coupled with WAQ (developed by WL | Delft Hydraulics),
3. Slib3D (developed by Rijkswaterstaat of the Ministry of Transport and Public Works of The Netherlands) coupled with WAQUA/TRIWAQ within SIMONA environment.

#### **DELFT3D - WAQ**

DELFT3D is a modelling suite that integrates the simulation of hydrodynamics (flow and waves), sediment transport, water quality and morphology. The various modules are coupled offline, i.e. by means of an intermediate file from which each module reads necessary data generated by one of the other modules. DELFT3D can be run in 3D as well as 2D (depth-averaged) mode. The module WAQ includes a large variety of water quality processes. A subset of WAQ is formed by SED which only addresses the transport of non-cohesive and cohesive sediment.

#### **DELFT3D - SED ON-LINE**

A special version of Delft3D is formed by DELFT3D SED ON-LINE, which computes simultaneously, i.e. at each numerical time step, hydrodynamics and sediment transports. This methodology avoids the generation of a (large) intermediate file and allows the simulation of sediment-fluid interaction. It employs state-of-the-art process formulations as described in Section 4.2. DELFT3D SED ON-LINE can be extended in future with improved process formulations. The software package will be used for the three-dimensional or two-dimensional (depth-averaged) modelling of the Lower Sea Scheldt. Boundary conditions will be prescribed at both ends of the Sea Scheldt, i.e. tidal discharges (incl. river run off) and suspended sediment concentrations at the upper boundary near Schelle and water levels, salinities and suspended sediment concentrations at the downstream boundary near Waarde.

#### **WAQUA/TRIWAQ coupled with WAQ**

SCALWEST2000 is a dedicated model for the Western Scheldt including the coastal zone (Voordelta) and the Sea Scheldt. It is based on the WAQUA software package and can only be used in 2D (depth-averaged) mode. The fine-grid version contains approximately 82,000 grid points. To allow the simulation of sediment transports it will be coupled with the DELFT3D module WAQ. The model can be run parallel on several processors to increase computational speed. Boundary conditions will be prescribed at the sea boundary (water

levels or tidal constituents, salinities and suspended sediment concentrations) and the river boundary (tidal discharges, incl. river run off, and suspended sediment concentrations).

### WAQUA/TRIWAQ coupled with SLIB3D

An alternative approach is the use of the SIMONA system in which WAQUA/TRIWAQ and SLIB3D are embedded, running in parallel mode. SLIB3D has some of the features of SED ON LINE and WAQ and can be used for relatively simple fine sediment transport computations. SLIB3D solves the advection-diffusion equation in a mass-conserving way on a curvi-linear grid with the following features:

- a numerical scheme with an efficient solver to account for large concentration gradients,
- water-bed exchange formulations based on threshold velocities in stead of critical shear stresses, and
- a parameterisation for the effect of waves in stead of an explicit wave description.

The areas of application of the aforementioned software packages are summarised in the table hereafter.

Software package	Area of application	Mode
DELFT3D-WAQ	Western Scheldt incl. Voordelta, Lower Sea Scheldt and upper reaches of the Scheldt river	2Dh
DELFT3D: SED ON-LINE	Lower Sea Scheldt	2Dh, 3D
WAQUA/TRIWAQ + WAQ	Western Scheldt incl. Voordelta, Lower Sea Scheldt and upper reaches of the Scheldt river	2Dh, 3D
WAQUA/TRIWAQ + SLIB3D	Western Scheldt incl. Voordelta, Lower Sea Scheldt and upper reaches of the Scheldt river	2Dh, 3D

## 4.4 Development phases

The DELFT3D SED ON-LINE model, equipped with state-of-the-art process formulations, is to be set up in conjunction with the WAQUA SCALWEST2000 model, as part of the SIMONA environment, coupled with WAQ. For both models grid schematisations of the areas already exist.

The original SCALWEST model has been calibrated for neap and spring tide conditions in 1996 and subsequently validated for average tidal conditions and storm conditions in 1996, however only with respect to hydrodynamics. Various modifications have been applied to the modelled area as well as the grid by the Ministerie van de Vlaamse Gemeenschap. After the 'deepening of the Sea Scheldt in 1999 the model was calibrated again using field data from May/June 2002.

The DELFT3D SED ON-LINE model for the Lower Sea Scheldt requires calibration and validation of the hydrodynamics and sediment transports. The acquisition of field data (see Chapter 5) is important. Prior to this, trial runs with the models may assist in further detailing the proposed measuring campaigns.

Results will be analysed as follows:

- Water movement and bed shear stresses with respect to large-scale transport
- Water movement and bed shear stresses with respect to small-scale transport
- Three-dimensional structure of the water movement (with the 3D model)
- Analysis of sediment transport pattern for marine and fluvial mud.

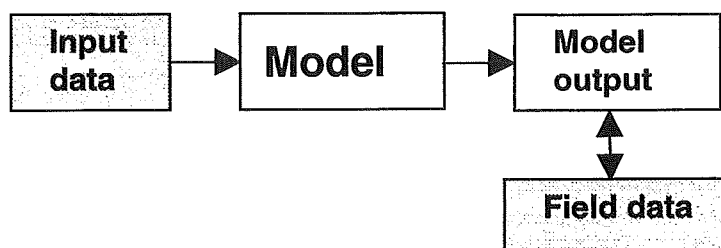
Following calibration and validation of the Delft3D model and the application of the model in answering managerial questions, new process formulations will have to be implemented. This activity may start by the beginning of 2005.

## 5 Data requirements

Data that are required for the models, as described in Chapter 4, can be subdivided in two categories<sup>2</sup>:

- data as part of the input and that is needed to run the model(s);
- data to compare output of the model(s) with field observations, which are needed during the process of calibration and verification.

This is schematically shown below:



Input data is needed (i) for the various process formulations of the model (e.g. settling velocity of mud, critical shear stresses etc.), (ii) to describe the initial state of the model (e.g. bathymetry, bed composition) and (iii) to prescribe the boundary conditions of the model (e.g. suspended sediment concentrations). The latter can also be derived from an overall model, which subsequently also demands input data and field data for calibration. If input data are not precisely known (which is generally the case), they have to be estimated and adjusted during calibration of the model. The calibration process requires field data, and the extent to which field data and model output coincides determines the performance of the model. Input data can be based on literature, laboratory measurements and field measurements; to assess the performance of the model during calibration and verification field observations are needed.

### Input data for process formulations

Input data for process formulations depend on the type of formulations incorporated in the model. More advanced modelling of processes, e.g. as part of Phase 2 of the model development, will require very specific model parameters. How to determine these parameters should be addressed in the future, if such a modelling approach is selected. Hereafter, attention is restricted to the state-of-the-art modelling during Phase 1. The processes, as listed in Par. 4.2, are given below and the method to acquire the various parameters is also indicated.

---

<sup>2</sup> In this chapter the attention is focused on data requirements for the cohesive sediment transport model.



Process	Type of process formulation	Input data for process formulations
flocculation	functional dependency on salinity (S), suspended sediment concentration (c) and turbulence (G)	$w_s = f(S, c, G)$ <ul style="list-style-type: none"> <li>to derive during calibration and from laboratory and field measurements</li> <li>aggregation and break-up parameters</li> </ul>
settling & hindered settling	functional dependency on suspended sediment concentration	$w_s = g(c)$ to derive during calibration and from laboratory and field measurements
gelling	output from flocculation model	
sediment-fluid interaction	explicitly modelled	gelling concentration $c_{gel}$
sediment-induced gravity currents regarding HCMS	explicitly modelled	gelling concentration $c_{gel}$
sediment-induced gravity currents regarding fluid mud	explicitly modelled	gelling concentration $c_{gel}$
sedimentation and siltation	<ul style="list-style-type: none"> <li>explicitly modelled</li> <li>computation of bed accumulation</li> </ul>	$D = w_s c_b$ bed density
consolidation	parameterisation of full consolidation equation	material functions for effective stress and permeability using a fractal approach
erosion and re-entrainment	<ul style="list-style-type: none"> <li>explicitly modelled with 'Partheniades' approach</li> <li>computation of bed erosion</li> </ul>	$E = M (\tau_b / \tau_e - 1)$ $M$ and $\tau_e$ from literature and adjustment during calibration.
bed boundary conditions and rheology	<ul style="list-style-type: none"> <li>bed density and bed strength</li> </ul>	from measurements
sand-mud mixtures	<ul style="list-style-type: none"> <li>modified erosion and sedimentation as function of the bed mud content</li> <li>computation of bed composition (two fractions)</li> </ul>	<ul style="list-style-type: none"> <li>sand and mud properties: sand grain size, settling velocities sand and mud, critical shear stresses and erosion rate mud</li> <li>critical mud content to distinguish between non-cohesive and cohesive behaviour</li> <li>density and mixing parameters of the bed</li> </ul>

## Data for calibration and verification

The accuracy of a model simulating cohesive sediment transport processes in the Lower Sea Scheldt is determined during the calibration and verification of the model. The comparison between model results and field observations should be done for the suspended sediment as well as the sediment accumulating on the bed; the temporal and spatial variation should be adequately reproduced by the model. This requires the following field data:

### *Suspended sediment*

Suspended sediment concentrations in a number of stations along the Lower Sea Scheldt on times scales of (i) a tidal cycle, (ii) on a spring-neap tidal cycle and (iii) on a seasonal time scale. Measurements may be done in fixed stations by means of turbidity sensors at various depths or with ADCP measurements from (moving) boats covering the whole cross-section. The former measurements will give spatially discrete data on long time scales (neap-spring tide and seasons) while the latter will result in spatially high resolution data on relatively short time scales (tide).

Apart from the sediment quantity (concentration) also the sediment quality (composition) is of importance. This requires analyses on the grain size distribution (specifically mud and silt fractions) and organic content.

Detailed ADCP measurements during a tidal cycle will, amongst others, supply information on density induced gravity currents, the vertical distribution due to soil-water exchange processes and the lateral distribution of suspended sediment due to secondary currents in river bends. Long-term measurements will show the variation of the location of the turbidity maximum during the neap-spring tidal cycle and due to variations in the river discharge. Also the effect of episodic events (storms) will be highlighted with these type of measurements.

Information on suspended sediment concentrations at the boundaries of the detailed model for the Lower Sea Scheldt is specifically needed to compare with the output of the overall model for the Scheldt estuary. The locations are near Schelle, at the upstream boundary of the detailed model, and at Waarde at the downstream boundary.

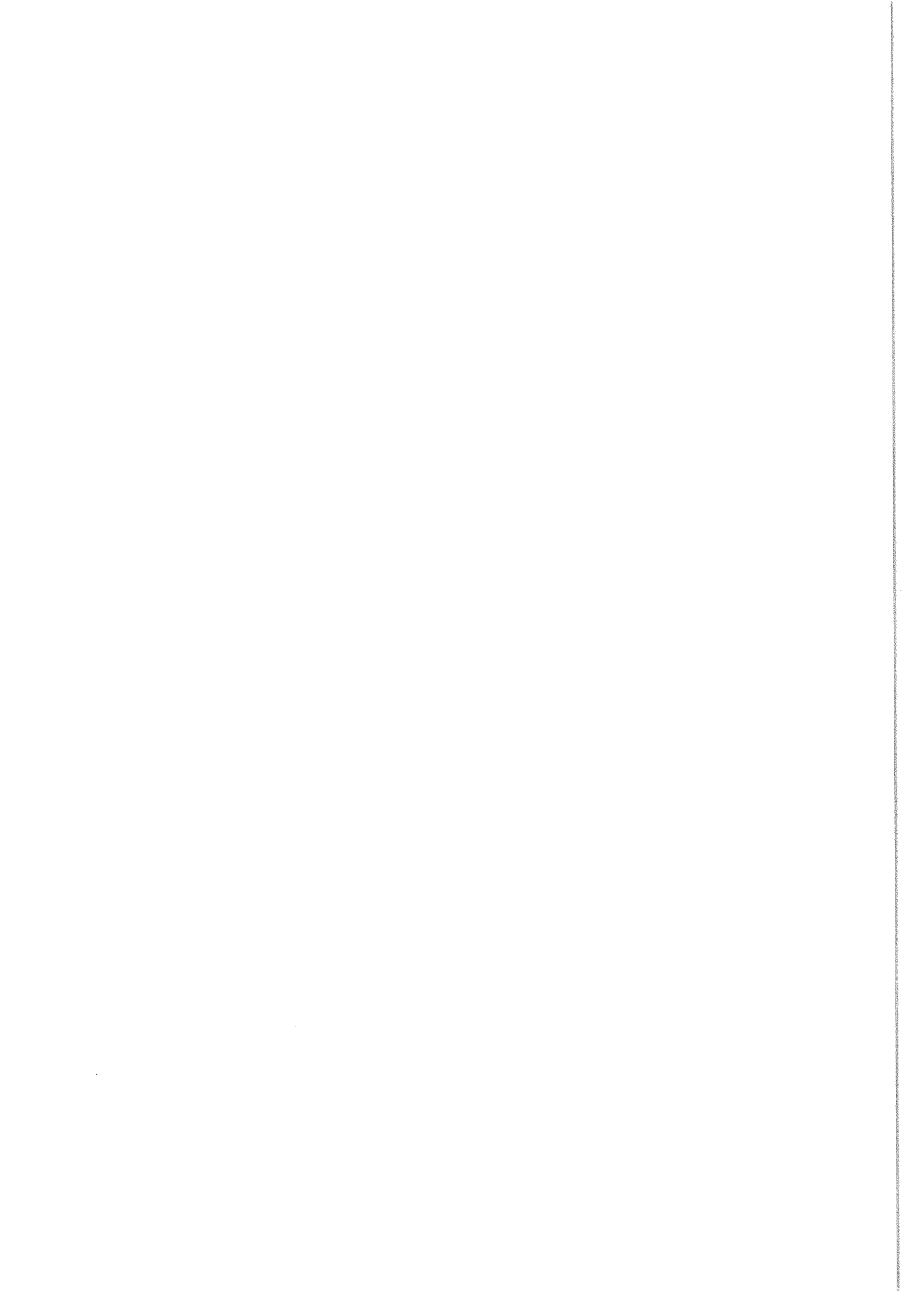
### *Bed sediment*

Information on the composition (grain size distribution, mud and clay fraction, bed density) and thickness of the upper layer of the bed is required. An accurate representation of the river bed as an initial condition for the simulation will reduce the spinning-up time of the model. Furthermore, historical data on siltation volumes (e.g. in the access channels to the Zandvliet and Kallo sluices) are needed to compare with model output. This includes information on in-situ bed density to allow for the recalculation from sediment volumes to sediment mass. Additional laboratory measurements should be done to characterise the bed sediment, such as: Atterberg Limits, CEC, rheological properties, organic content and mineralogy. Attention should also focus on the bed composition of the intertidal areas and salt marshes as this may differ from the bed composition of the river bed.

The required data, as described above for suspended as well as bed sediment, are essentially the same for the detailed model for the Western Scheldt and the overall model which supplies the appropriate boundary conditions.

## References

- Claessens, L., H. Belmans, 1984, Overzicht van de getijwaarnemingen in de Zeescheldebekken gedurende de periode 1971-1980. *Tijdschrift van de Openbare Werken van België*, nr. 3.
- De Brouwer, J.F.C., 2002, "Dynamics in extracellular carbohydrate production by marine benthic diatoms", PhD-thesis, Katholieke Universiteit Nijmegen; Netherlands Institute of Ecology.
- Fettweis, M., 1995, Modelling currents and sediment transport phenomena in shelf seas and estuaries, PhD thesis, KU Leuven.
- Ham, R. van der, 1999, Turbulent exchange of fine sediments in tidal flow, PhD-thesis, Delft University of Technology, Faculty of Civil Engineering and Geotechnical Sciences.
- IMDC (International Marine and Dredging Consultants), 1993, Gedrag van Particulair materiaal in het Schelde estuarium, Final Report for BMM (Ministerie van Volksgezondheid en Leefmilieu).
- Ledden, M. van, 2003, Sand-mud segregation in estuaries and tidal basins, Ph.D thesis, Technical University of Delft.
- Malcherek, A., 1995, Mathematische Modellierung von Strömungen und Stofftransportprozessen in Ästuaren, Dissertation, Institut für Strömungsmechanik und Elektronisch Rechnen im Bauwesen der Universität Hannover, Bericht Nr. 44/1995 (in German).
- Salden, R.M., D.C. van Maldegem, 1998, Het effect van slibverwijdering in de Beneden Zeeschelde op de waterkwaliteit en slibhuishouding in de Westerschelde, RIKZ Middelburg, Rapport RIKZ 98.015.
- Schelde Informatie Centrum (SIC), 1999, De Schelde Atlas – een beeld van een estuarium.
- Taverniers, E., 2000, Beneden-Zeeschelde: Slibbalans 1999, Ministerie van de Vlaamse Gemeenschap, Departement Leefmilieu en Infrastructuur, Administratie Waterwegen en Zeewezen, Afdeling Maritieme Schelde, Antwerpen, rapport, AMS-2000-04.
- Van Eck, G.T.M., N. De Pauw, M. Van Langenbergh and G. Verreet, 1991, Emissies, gehalten en gedrag van effecten van (micro)verontreinigingen in het stroomgebied van de Schelde-estuarium, Water 60, pp. 244-256.
- Van Maldegem, D., 1993, De slibbalans van het Schelde-estuarium, RIKZ Middelburg, GWAO-91.081.
- Verlaan, P.A.J., 1998, Mixing of marine and fluvial particles in the Scheldt estuary, Ph.D., Delft University of Technology.
- Wang, Z.B., M.C.J.L. Jeuken, H. Gerritsen, H.J. de Vriend, B.A. Kornman, 2002, Morphology and asymmetry of the vertical tide in the Westerschelde estuary, *Continental Shelf Research*, 22, 2599-2609.
- Wartel, S., G.T.M. van Eck, 2000, Slibhuishouding van het Schelde estuarium, Koninklijk Belgisch Instituut voor Natuurwetenschappen / RIKZ.
- Widdows, J. and M. Brinsley, 2002, Impact of biotic and abiotic processes on sediment dynamics and the consequences to the structure and functioning of the intertidal zone, *Journal of Sea Research*, 48, 43-156.
- Winterwerp, J.C., 1998, A simple model for turbulence induced flocculation of cohesive sediment, *IAHR, Journal of Hydraulic Engineering*, 36 (3) 309-326.
- Winterwerp, J.C., 2001, Stratification of mud suspensions by buoyancy and flocculation effects, *Proceedings of the XXIX IAHR Congress, September 2001, Beijing, China, Theme D*, 235-241.
- Winterwerp, J.C. 2002, On the flocculation and settling velocity of estuarine mud, *Continental Shelf Research*, 22, 1339-1360.
- Winterwerp, J.C., Z.B. Wang, J.A. van Pagee, F. Mostaert, Y. Meersschaut, T. De Mulder, J. Claessens, 2002, Morphological changes in the Scheldt estuary and its consequences on hydrodynamics. Submitted to *Hydrobiologica*, *Proceedings ECSA local meeting Oct. 2002. Ecological structures and functions in the Scheldt Estuary*.
- Winterwerp, J.C., T. van Kessel, 2002, Siltation by sediment-induced density currents, *PECS 2002, Hamburg*.
- Winterwerp, J.C., 2003, "The transport of fine sediment in shallow basins" WL | delft hydraulics, report Z3506.
- Winterwerp, J.C., W.G.M. van Kesteren, 2004, *Cohesive Sediment in the Marine Environment (in preparation)*.
- Wollast, R., A. Marijns, 1981, Evaluation des contributions de differentes sources de matières en suspension a l'envasement de l'Escaut, Report to: Ministry of Public Health and Environment, 152 p



## A Parameterisation of flocculation

We start our parameterisation with the Lagrangean flocculation model (e.g. Winterwerp, 1998, 2002), assuming  $D_e \propto c$  and  $D_e = \lambda_0$ :

$$\frac{dD_f}{dt} = \frac{k_A}{n_f} c G D_f^{4-n_f} - \frac{k_B}{n_f} G^{3/2} (D_f - D_p) D_f^{4-n_f} \quad (\text{A.1})$$

in which  $D_f$  is the floc size (or its median diameter),  $D_p$  is the diameter of the primary particles from which the flocs are formed,  $n_f$  is the fractal dimension of the flocs,  $c$  is the suspended sediment concentration by mass,  $G$  ( $\equiv \sqrt{\epsilon/\nu}$ ) the shear rate at the smallest turbulence length scales (e.g. the Kolmogorov length scale  $\lambda_0$ ) and in which we have defined a dimensional aggregation parameter  $k_A$  [ $m^{n_f}/kg$ ] and floc break-up parameter  $k_B$  [ $s^{1/2}/m^{4-n_f}$ ]. In the following we assume that  $D_f \gg D_p$ . The equilibrium solution to (A.1) in that case reads:

$$D_e = \frac{k_A c}{k_B \sqrt{G}} \quad (\text{A.2})$$

where  $D_e$  is the equilibrium floc size. Further, we define a time scale parameter  $T'$ :

$$T' = \left( k_B G^{3/2} D_e^{4-n_f} \right)^{-1} \quad (\text{A.3})$$

So we can rewrite (A.1) as:

$$\frac{dD_f}{dt} = \frac{k_B G^{3/2} D_f^{4-n_f}}{n_f} [D_e - D_f] = \frac{D_e - D_f}{n_f T'} \quad (\text{A.4})$$

which shows that the flocculation process is governed by the time scale parameter  $T'$ . This observation has important implications for the flocculation behaviour in marine conditions. Flocs settle continuously due to gravity and are remixed by turbulence. Hence, they experience varying hydrodynamic conditions (shear rates) during their journey through the water column. This implies that the ratio between flocculation time and residence time in a specific turbulent environment becomes an important parameter.

This can be quantified by considering a situation where the turbulence field is homogeneous over the water depth, as can be realised in a settling column, for example. The mean residence time  $\tau$  for all particles in the water column with initial height  $Z_0$  above the bottom of the water column can be obtained from:

$$\int_0^\tau w_s dt = \alpha'' \int_0^\tau D_f^{n_f-1} dt = Z_0 \quad (\text{A.5})$$

in which  $w_s$  is the settling velocity and  $\alpha'' = \alpha' g \Delta D_p^{3-n_f} / \nu$  (e.g. Winterwerp, 1998), in which we have used:

$$w_s = \frac{\alpha}{18\beta} \frac{(\rho_s - \rho_w)g}{\mu} D_p^{3-n_f} \frac{D_f^{n_f-1}}{1+0.15Re_p^{0.687}} \quad (\text{A.6})$$

assuming  $Re_p$  is small. We can solve (A.1) (c.q. (A.4)) analytically using (A.5) for  $n_f = 2$  and 2.5:

$$D_\tau = \frac{D_e}{1 + \left(\frac{D_e}{D_o} - 1\right) \exp\left\{-\frac{Z_0}{n_f w_{s,e} T'}\right\}} \quad (\text{A.7a})$$

$$\approx D_e \left[ 1 - \frac{D_e - D_o}{D_o} \exp\left\{-\frac{Z_0}{n_f w_{s,e} T'}\right\} + \dots \right] \quad \text{for } n_f = 2 \quad (\text{A.7b})$$

and

$$D_\tau = D_e \left[ 1 - \frac{D_e - D_o}{D_e} \exp\left\{-\frac{Z_0}{n_f w_{s,e} T'}\right\} \right] \quad \text{for } n_f = 2.5 \quad (\text{A.8})$$

Note that the expansion (A.7b) is not valid for  $\lim Z_0 \rightarrow 0$ , c.q.  $\lim T' \rightarrow \infty$  as  $D_e > D_o$  in general. Equ. (A.1) cannot be solved analytically for other values of  $n_f$ . However, (A.7) and (A.8) suggest that a general form of the solution to (A.1) can be written as:

$$D_\tau = D_e - k_2 (D_e - D_o) \exp\left\{-\frac{Z_0}{n_f w_{s,e} T'}\right\} \quad (\text{A.9})$$

We can interpret  $D_\tau$  as the maximum floc size that can be attained in the time period that the flocs reside in the turbulent field with dimensions characterised by  $Z_0$ , i.e.  $D_\tau = D_{max}$ . A characteristic measure for  $Z_0$  is the water depth  $h$ . The initial floc size  $D_o$  can be interpreted as the smallest floc size that occurs in the water column, and we assume that that is the equilibrium floc size for the highest shear stresses in the water column, i.e. near the bed. Thus  $D_o = D_{min}$ , which is found from:

$$D_o = D_{min} = \frac{k_A c}{k_B \sqrt{G_{max}}} \quad (\text{A.10})$$

This yields:

$$D_{max} = \frac{k_A c}{k_B \sqrt{G}} - k_2 \left( \frac{k_A c}{k_B \sqrt{G}} - \frac{k_A c}{k_B \sqrt{G_{max}}} \right) \exp\left\{-\frac{k_A^{2n_f-5} h c^{2n_f-5}}{\alpha' n_f k_B^{2n_f-4} G^{n_f-1}}\right\} \quad (\text{A.11})$$

So we obtain the four parameter formula in which the coefficients  $k_1$ ,  $k_2$ ,  $k_3$  and  $n_f$  have to be determined empirically from field data (N.B.  $k_2 \approx 1$  and  $2 \leq n_f < 3$ ):

$$D_{\max} = k_1 \frac{c}{\tau} - k_2 \left( k_1 \frac{c}{\tau} - k_1 \frac{c}{\tau_{\max}} \right) \exp \left\{ -\frac{k_3}{n_f} \frac{hc^{2n_f-5}}{\tau^{n_f-1}} \right\} \quad (\text{A.12})$$

in which  $\tau$  is the local and  $\tau_{\max}$  the maximal shear stress in the water column. With the use of equ. (A.6), equ. (A.12) can also be written as:

$$W_{s,\max} = \left[ k_4 \frac{c}{\tau} - k_2 \left( k_4 \frac{c}{\tau} - k_4 \frac{c}{\tau_{\max}} \right) \exp \left\{ -\frac{k_3}{n_f} \frac{hc^{2n_f-5}}{\tau^{n_f-1}} \right\} \right]^{n_f-1} \quad (\text{A.13})$$

The fitting procedure can be simplified by considering the right-hand part of the data, i.e. at large  $\tau$ , where equilibrium is expected.

Note that we cannot solve (A.1) analytically for  $D_e$  or  $W_{s,e} \propto c^r$ ,  $r \neq 1$ , and we have to guess that the solution will have a form like (A.8), in which we include the  $r \neq 1$  dependency in  $D_e$  (c.q.  $W_{s,e}$ ) only. Of course in that case, a fifth calibration coefficient (e.g.  $r$ ) has to be found.

